Report 3281

BOW-THRUSTER JET FLOW

NAVAL SHIP RESEARCH AND DEVELOPMENT CENTER
Washington, D.C. 20007

BOW-THRUSTER JET FLOW

by
John L. Beveridge

DEPARTMENT OF HYDROMECHANICS

RESEARCH AND DEVELOPMENT REPORT

March 1970

Report 3281

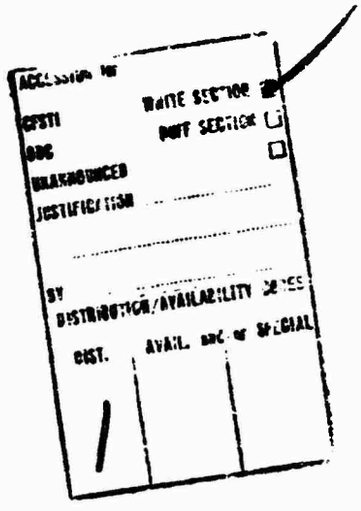

The Naval Ship Research and Development Center is a U.S. Navy center for laboratory effort directed at achieving improved sea and air vehicles. It was formed in March 1967 by merging the David Taylor Model Basin at Carderock, Maryland and the Marine Engineering Laboratory at Annapolis, Maryland. The Mine Defense Laboratory, Panama City, Florida became part of the Center in November 1967.

Naval Ship Research and Development Center
Washington, D.C. 20007

DEPARTMENT OF THE NAVY
NAVAL SHIP RESEARCH AND DEVELOPMENT CENTER
WASHINGTON, D. C. 20007

BOW-THRUSTER JET FLOW

by

John L. Beveridge

March 1970

Report 3281

TABLE OF CONTENTS

LIST OF FIGURES

NOTATION

A	Cross-sectional area of duct
B	Maximum beam
C_p	Pressure coefficient P/q
D	Duct diameter
g	Acceleration due to gravity
h	Velocity head
K_F	Body-force coefficient $\frac{T}{\rho A U_j^2}$
L	Body length
N	Body pitching moment (positive bow up)
N'	Body pitching-moment coefficient $\frac{N}{\rho A U_j^2 X_T}$
P	Net static pressure
q	Stagnation pressure $\frac{\rho}{2} U_\infty^2$
q_j	Jet dynamic pressure $\frac{\rho}{2} U_j^2$
R	Offset of meridian profile
R_{n_D}	Duct Reynolds number
R_{n_B}	Body Reynolds number
r	Nondimensional offset of meridian profile R/L
T	Body force delivered by bow thruster (in direction of duct axis)
U_j	Duct mean velocity
U_∞	Undisturbed fluid velocity
$\forall$	Duct volume flow rate
X_T	Distance of duct axis from center of gravity
x,y,z	Nondimensional coordinates (longitudinal, lateral, normal) in terms of length L, origin at the bow
$\Delta C_p'$	Pressure coefficient $\Delta P/q_j$
θ	Vectorial angle
ν	Kinematic viscosity
ρ	Mass density of fluid
ϕ	Flow coefficient $\forall / B^2 U_\infty$

ABSTRACT

Interaction between the ambient flow of a hull and bow-thruster inflow and outflow is examined theoretically and experimentally. Pressure distributions for duct inflow were derived by potential-flow techniques, and wind-tunnel pressure tests and flow-visualization experiments were conducted to determine the characteristics of duct outflow. Generalized and specific results are presented and discussed for two sizes of circular ducts operating over a range of ratios of free-stream velocity to jet velocity.

ADMINISTRATIVE INFORMATION

This work was performed and funded under Subproject SF35.421.006 (NSRDC Problem 526-197) of Naval Ship Systems Command Task 1713.

INTRODUCTION

Measurements of body force and body moment by several investigators[1-4] have shown that at a forward vehicle speed the control effectiveness of conventional transverse bow thrusters is reduced compared to the static case. Measurements reported by Stuntz and Taylor[5] do not show this trend; however, their tests were conducted on a partial model of a surface ship that had only the forward three stations and so surface forces were not completely represented. Calculations of the ratio of body moment to body force (with static data deducted) have shown that the line of action of hull suction force moves aft with forward speed.[1] Impeller thrust measurements by Taniguchi[3] and measurements of impeller torque by Feldman[4] indicate that the contribution of the ducted-propeller thrust to the body total force is hardly affected by forward speed. That this is so has been reasoned by Chislett and Björheden.[1]

It has been widely hypothesized from previously described information that the loss in both body-force and body-turning moment results from the suction forces and their center of action on the hull caused by mutual interaction between the thruster jet flow and the ambient flow. The exact flow mechanism of this interaction cannot be determined from

---

[1]References are listed on page 46.

gross force measurements but requires detailed flow studies. Therefore, this report discusses the flow mechanism associated with jets, as typified by circular bow thrusters, issuing approximately perpendicular to the main stream.

A search of the literature has revealed that the primary interest in this kind of flow phenomenon has been in the aeronautical field. The flow of a jet directed normal to a uniform steady crosswind is considered in the solution of the practical problem of discharge of waste gases from chimney stacks.[6] The problem involved in using jets to provide the necessary lifting thrust for vertical takeoff of aircraft led Jordinson[7] to conduct experiments on the outflow of an air jet from an orifice in a plane wall into an airstream. There is similarity between these flow problems and the effect of forward vehicle speed on the action of bow thrusters. However, the inflow and outflow of bow thrusters are further complicated by the fact that the duct opening is located on a curved surface and by the presence of a nonuniform surrounding flow.

To determine the flow phenomenon, a parametric flow study was performed on a specific hull configuration for which some aspects of the control effectiveness of bow thrusters had been evaluated.[4] The preliminary design for the deep-submergence rescue vessel (DSRV) was chosen for this purpose because (1) captive-model tests[4] made to determine the stability and control characteristics of this vessel indicated a considerable "falloff" of normal (vertical) force with increasing forward speed, (2) detailed force and moment data were available for this model, and (3) the basic flow mechanism should essentially be independent of hull shape. Since the free turbulent-shear flow of the turbulent jet issuing normal to the free stream is inherently complex, the need for an experimental investigation of bow-thruster exit flow is obvious. Consequently, a 1/3-scale groundboard model of the DSRV was constructed for tests in the NSRDC 8- x 10-foot subsonic wind tunnel. Flow-visualization (smoke) tests and pressure-distribution tests were made of the jet exit flow for 2- and 4-inch-diameter circular ducts when the ratio of free-stream velocity to jet velocity was varied. Duct-entrance flow was studied by means of appropriate potential flow models.

The important features and details of both the theoretical and experimental approach are given, and the computational and experimental results are presented and discussed.

PRINCIPAL CONSIDERATIONS

The action of a bow thruster at forward vehicle speed depends on the parameter U_∞/U_j which is the ratio of free-stream velocity to the duct exit velocity.* Figure 1 shows the predicted body normal-force coefficient and body pitching-moment coefficient due to a ducted thruster as a function of U_∞/U_j for a DSRV configuration. The curves are estimated for a single vertical ducted-thruster unit from experimental data reported by Feldman[4] and are presented to provide qualitative data for discussion.

A study of bow-thruster jet flow can be logically divided into two parts, the duct inflow (entrance) and the duct outflow (exit). Duct inflow can be assumed to be essentially inviscid and therefore approximated by potential flow solutions. However, the complexity of the free turbulent-shear flow associated with the duct outflow requires an experimental investigation. Since the duct entrance flow can be reasonably approximated by a potential flow model, and computer programs are available at this Center to handle this type of flow problem, an analytical study of duct inflow has been made. The calculations were performed on the LARC computer at the Center using the Douglas-Neumann method.[8] This method is well known, and the numerical details, assumptions, and limitations will not be discussed.

The present experimental outflow studies were conducted on a ground-board model without appendages (Figure 2). Relative to Figure 1, it is hypothesized that three distinct flow regimes occur as follows:

1. The low velocity ratio region where the duct outflow remains essentially perpendicular to the hull with an effective turning moment.

---

*Note that this form of the parameter is preferred to the inverse ratio which becomes infinite at zero ship speed.

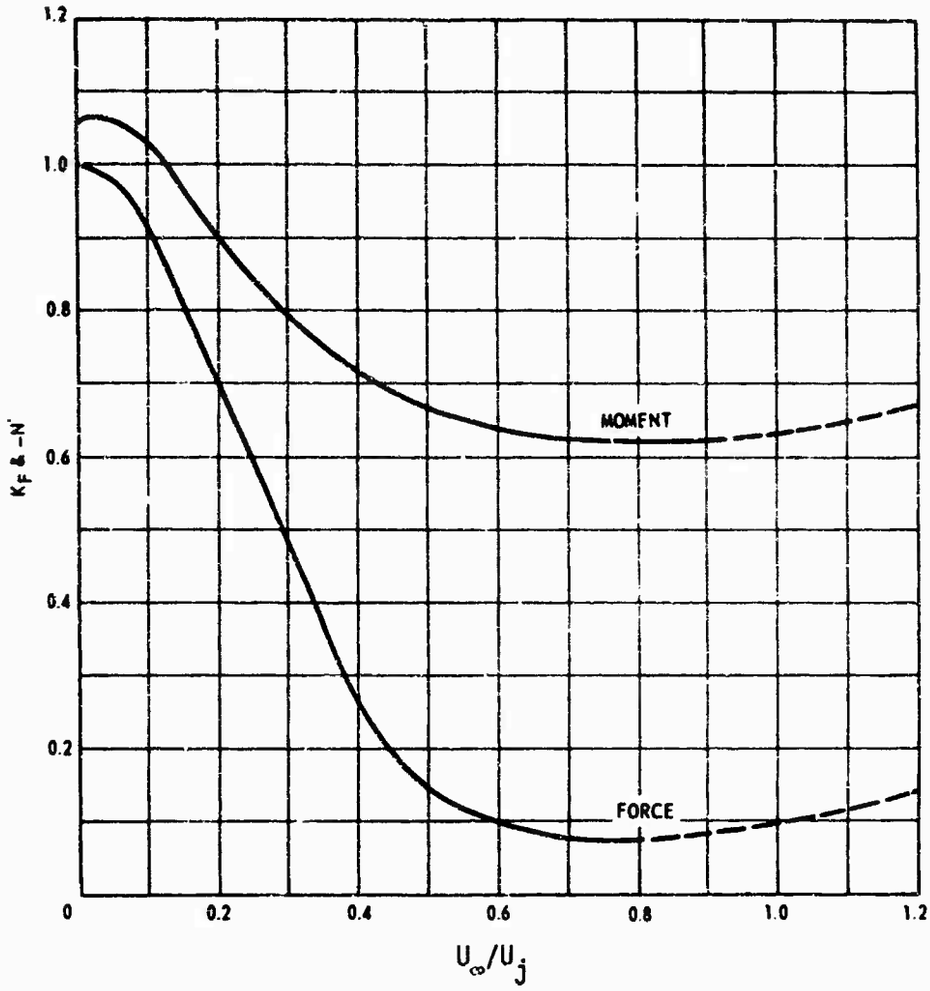

Figure 1 - Estimated Body-Force and Body-Moment Coefficients for a Submersible with a Bow Thruster

2. A critical range of U_∞/U_j for intermediate bending of the thruster jet with a considerable reduction in effectiveness of the turning moment.

3. A high velocity ratio region (not covered by the experimental data of Figure 1) where the thruster jet is greatly deflected and extends aft in close proximity to the hull with significant recovery of the turning moment.

It has been suggested that the relatively smaller loss in body-turning moment compared to body force is apparently caused by the progressively aft movement of the center of action of the suction forces. The suction force could eventually move aft of the center of gravity and even cause a favorable turning couple. It is apparent that a complete mapping of the pressure defect due to thruster jet flow is required to fully correlate pressure distribution and hull suction-force distribution. This circumstance arises because the precise hull area over which the thruster jet outflow and inflow diffuses must be determined as a function of U_∞/U_j. No attempt will be made here to do this. The shape of the curves of Figure 1 are highly dependent on both hull geometry and thruster size and location. The Chislett[1] experiments with a surface ship covered velocity ratios U_∞/U_j to approximately 1.6 and showed complete recovery of the turning moment.

MODEL CONFIGURATION AND TEST ARRANGEMENT

NSRDC Model 5166 is a 14.42-foot half-body of revolution that is constructed of white pine with the same offsets (Table 1) as the 1/3-scale DSRV model of Reference 4. Figure 2 shows Model 5166 installed on a ground board for flow tests in the NSRDC 8- x 10-foot subsonic wind tunnel. The centerline of the duct is located 19.0 inches aft of the bow. Full duct length of 29.35 inches was achieved by extending the duct below the ground board as shown in Figure 3. Interchangeable ducts of 2 and 4 inches in diameter were provided to investigate the effect of duct size. A removable extension three duct diameters in length (shown in Figure 2) could be attached to the 2-inch-diameter duct.

A constant-speed centrifugal fan (Figure 4) was used to obtain duct flow. At 3400 rpm, the fan capacity is 760 cubic feet per minute with a

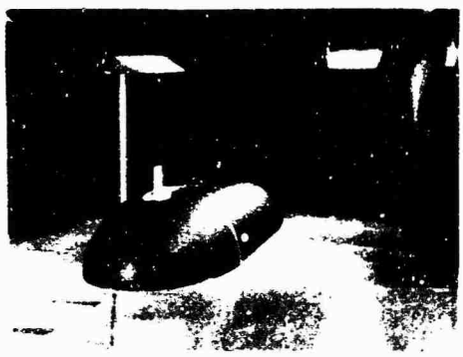

Figure 2 - Model 5166 Installed on Ground Board in NSRDC Subsonic Wind Tunnel

Figure 3 - Extension of Duct below Ground Board to Obtain Full Duct Length

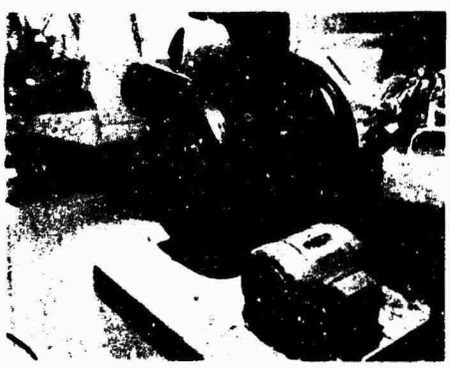

Figure 4 - Blower for Thruster-Duct Flow with Smoke Generator for Smoke Injection into Inlet

static pressure of 5 inches of water across the fan. A damper valve on the discharge line was used to regulate the flow. Smoke for the flow-visualization tests was produced by a commercial smoke generator and was introduced into the duct system at the blower intake. For the pressure-distribution tests, a series of piezometer taps was installed along the top meridian of the model from 2 to 90 percent of the model length. Piezometer taps were also installed around the girth of the hull at the duct centerplane. These taps surveyed a section from 10 to 60 degrees port and starboard, measured from the top.

POTENTIAL-FLOW ANALYSIS FOR DUCT ENTRANCE

Duct inflow and its effect on the pressure distribution on and near the hull surface was studied by means of a potential-flow model, using a method attributable to Hess and Smith.[8] Calculations were performed to obtain the pressure distribution on the duct-entrance side of the hull for a 4-inch duct at velocity ratios U_∞/U_j of 0.2, 1.0, and 2.0. The pressure distribution without a duct was also calculated. The entire body and duct configuration is mathematically represented in this method, but only the flow on the duct-entrance side of the hull is reasonably approximated by a potential-flow model.

A duct is really an interior flow problem; therefore, both ends are closed by a mathematical (imaginary) surface across the openings. Zero normal velocity is specified everywhere on the hull surface except at the duct ends where a nonzero uniform normal velocity is specified. Any distribution of normal velocity can be specified on the surfaces across the ends of the duct consistent with the principle of continuity. However, for the present case, a precise distribution across the duct entrance is not known a priori. In any event, it seems likely that at points away from the duct entrance--and these are of most interest here--the velocity induced by the duct total inflow is not very sensitive to this local condition.

Shaub and Cockshutt[9] mapped some streamlines for the potential flow into a normal inlet using conformal transformation methods that gave the potential flow into a quasi-circular two-dimensional inlet. It must be

remembered that the DSRV hull surface is not a plane wall. These streamline patterns are reproduced in Figure 5 where the changing flow with the ratio U_∞/U_j is beautifully pictured. The effect of duct inlet-lip radius R/D is also shown. Figure 5 gives a much clearer impression of the physical entrance flow than a word description could.

Figures 6 through 10 summarize all the calculated pressure-distribution results with duct inflow. Figure 6a gives curves of the pressure coefficient C_p along the top meridian versus nondimensional body length x for the no-duct case and for a duct with U_∞/U_j ratios of 0.2, 1.0, and 2.0. Two expected results may be observed from the curves of Figure 6a. First, thruster inflow has a pronounced effect on the hull pressure distribution near the duct entrance. When compared to the no-duct case, skewness in the curves is apparent, with a decrease in pressure upstream of the duct and an increase in pressure downstream of the duct. Second, the extent of thruster influence is quite limited, namely, upstream to $x \simeq 0.05$ and downstream to $x \simeq 0.30$. Figure 6b shows the pressure defect $\Delta C_p = (C_p)_{U_j} - (C_p)_{U_j=0}$ as a function of x for $U_\infty/U_j = 0.2$ and 1.0. A cancelling effect on the hull-surface forces due to the duct inflow-pressure defect is indicated between the upstream and downstream region. However, any net surface force near the duct entrance would produce a change in body-turning moment about the center of gravity.

Figure 7 shows the circumferential variation of the pressure coefficient along the hull girth at the duct location with $U_\infty/U_j = 0.2$. About 40 degrees away from the duct axis, a value $C_p \simeq -0.3$ reached; this is essentially the no-duct pressure coefficient shown in Figure 6a. The flow shown in Figure 8 for $U_\infty/U_j = 0.2$ along a 45-degree meridian gives C_p values almost identical to those for the no-duct curve in Figure 6a. Offbody pressure data are shown in Figures 9 and 10 for points along a line at z = 0.11 and 0.15 in the x-z plane. Distance of any point from the hull surface may be found by using Table 1. These curves are of academic interest but are shown for the sake of completeness.

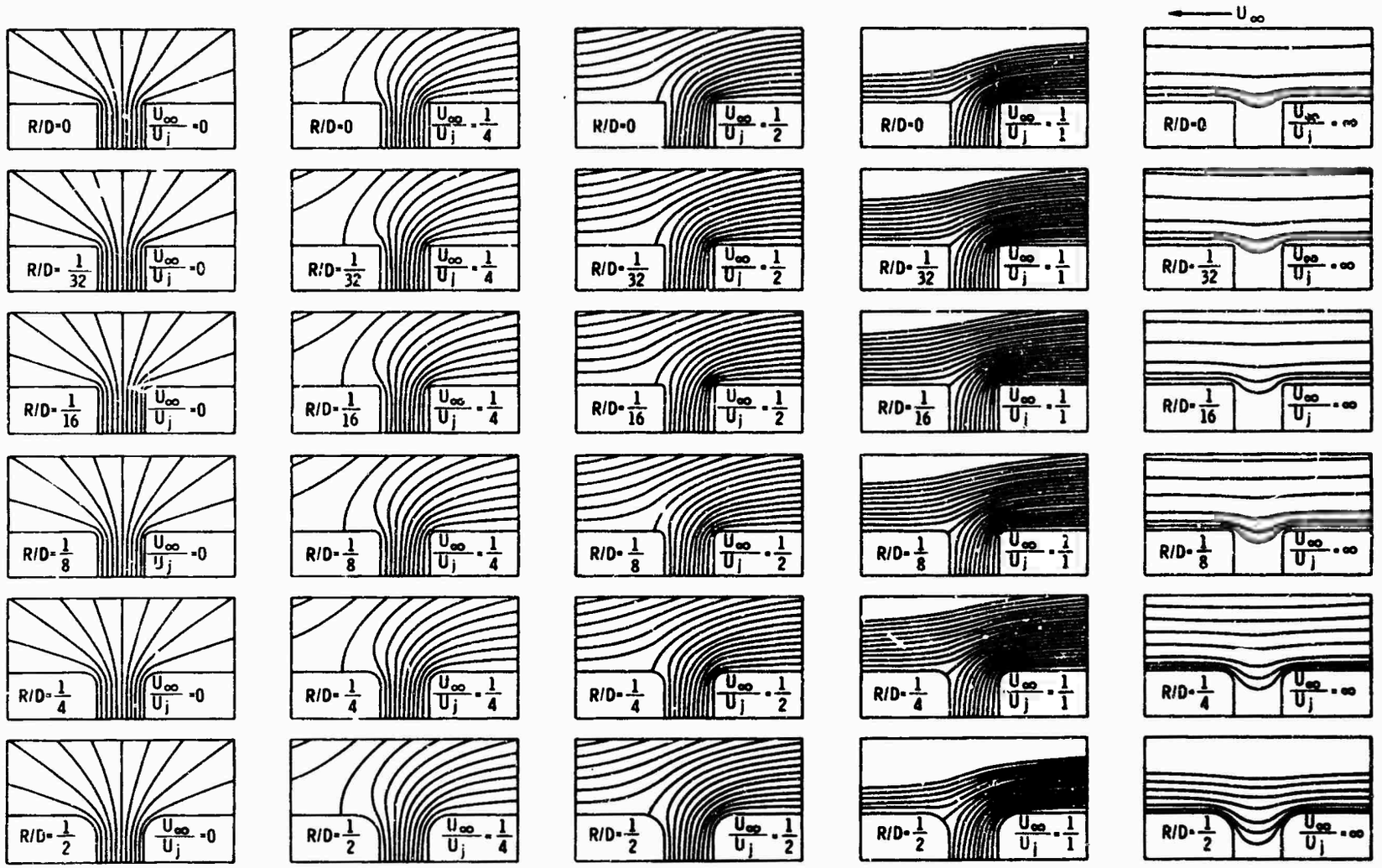

Figure 5 - Streamline Patterns, Inflow

(Reproduced from Reference 9 by permission of the publisher)

Figure 6 - Pressure Distribution along Top Meridian and Associated Pressure Defect for Duct Inflow of 4-Inch Duct

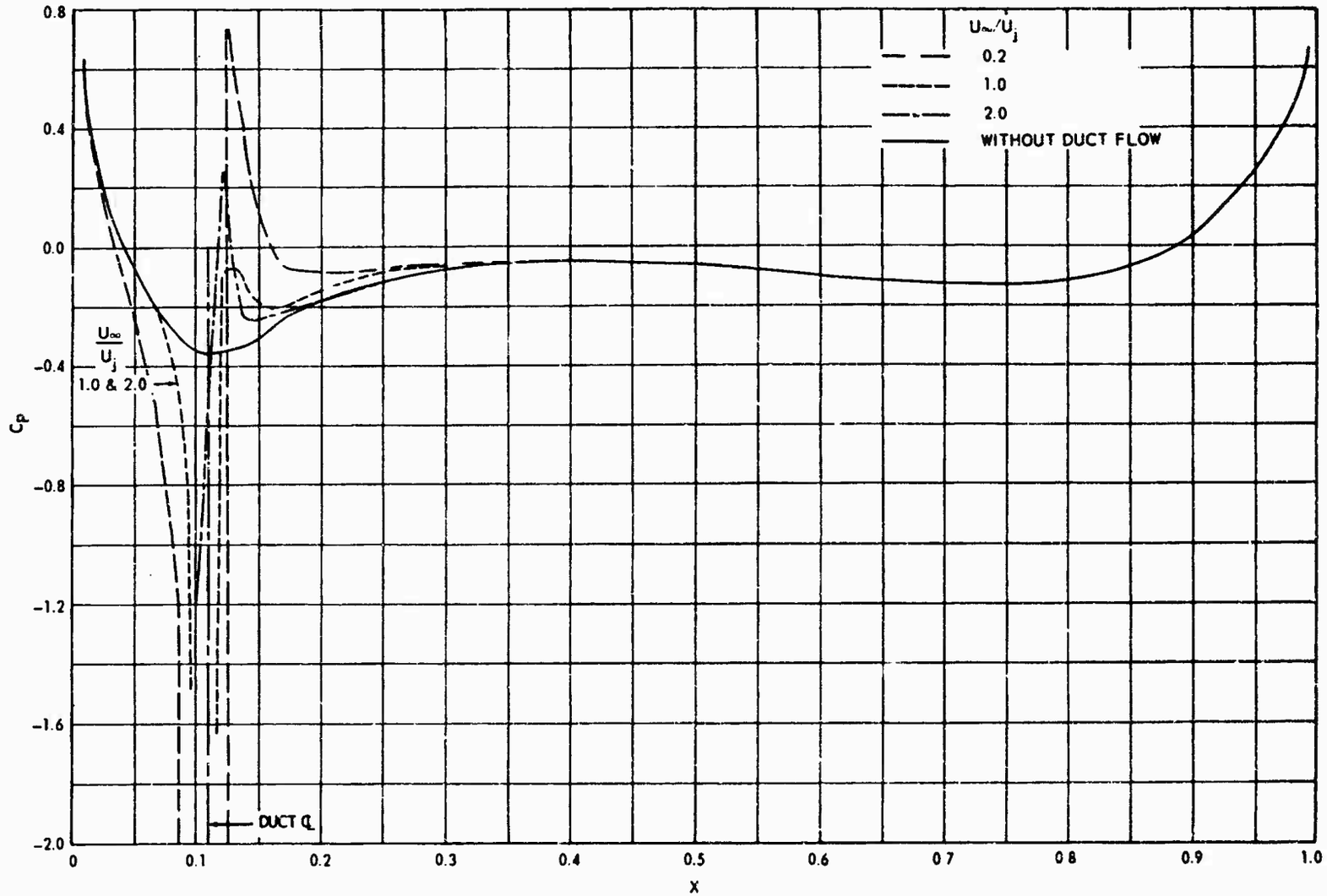

Figure 6a - Pressure Distribution

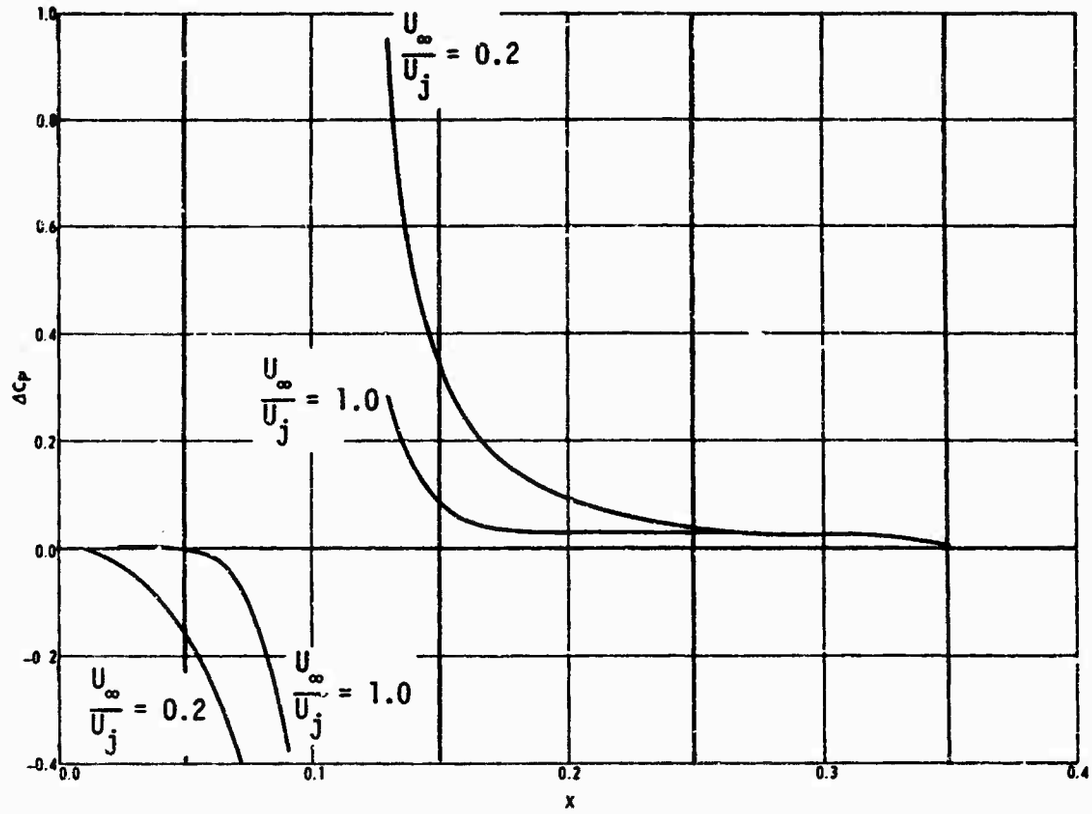

Figure 6b - Pressure Defect

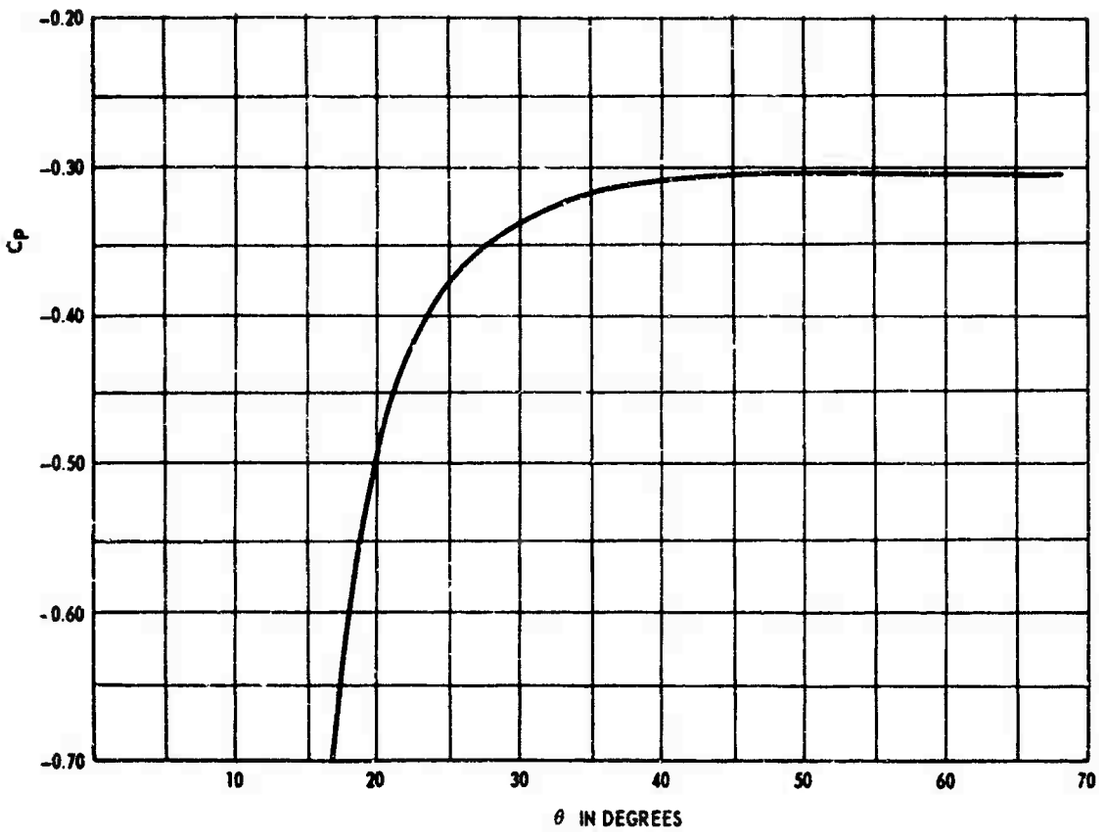

Figure 7 - Circumferential Variation for Duct Inflow of 4-Inch Duct at x = 0.107, U_∞/U_j = 0.2

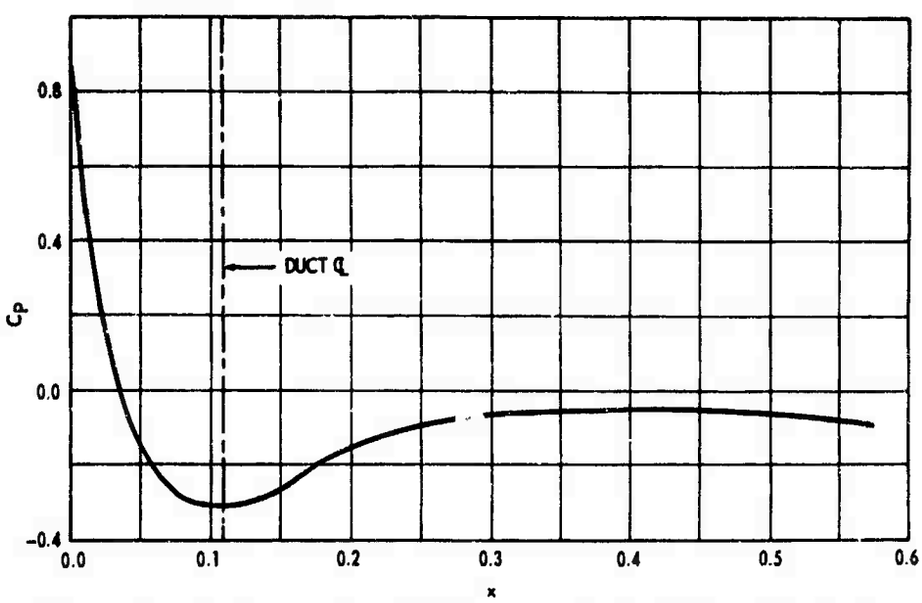

Figure 8 - Pressure Distribution along 45-Degree Meridian, Duct Entrance Flow for 4-Inch Duct at U_∞/U_j = 0.2

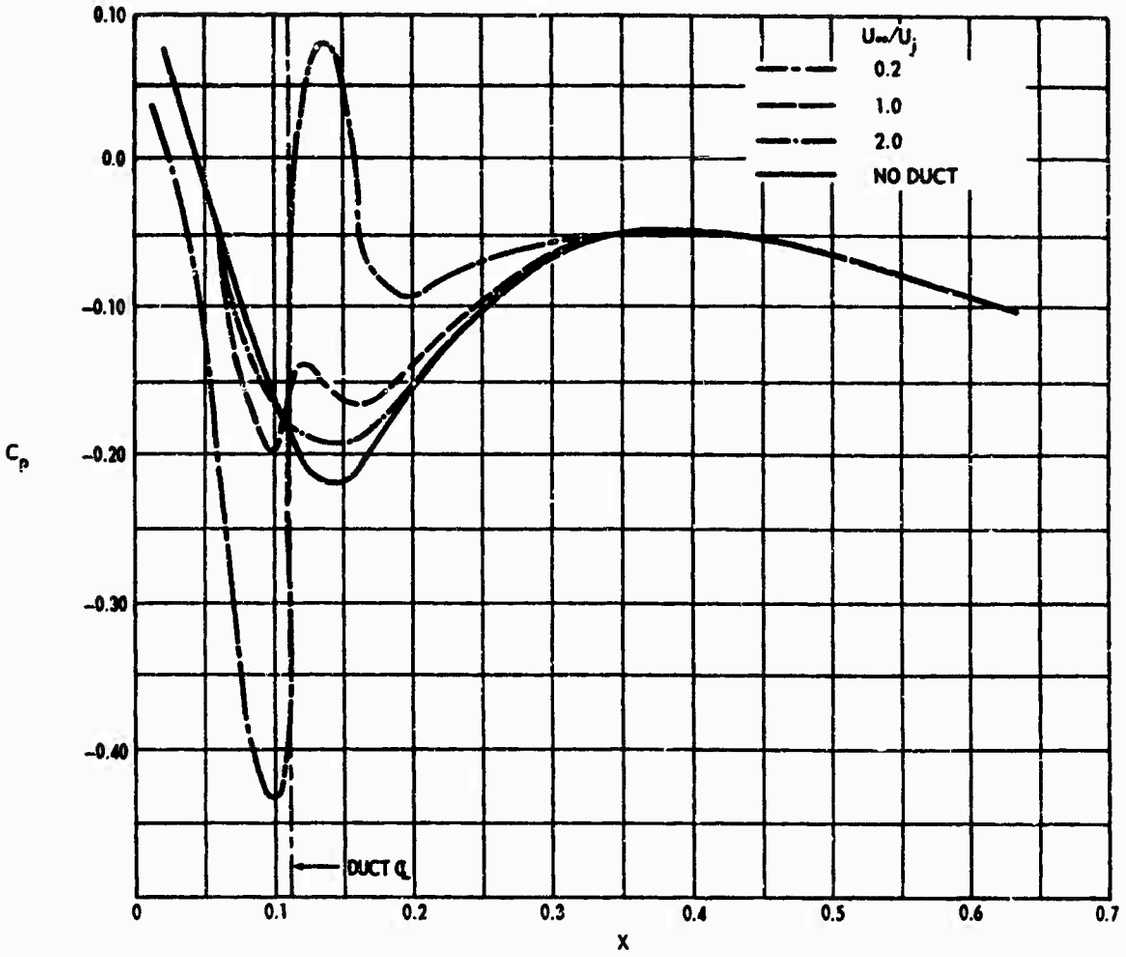

Figure 9 - Pressure Distribution off Body, Duct Entrance Flow for 4-Inch Duct at y = 0, z = 0.11

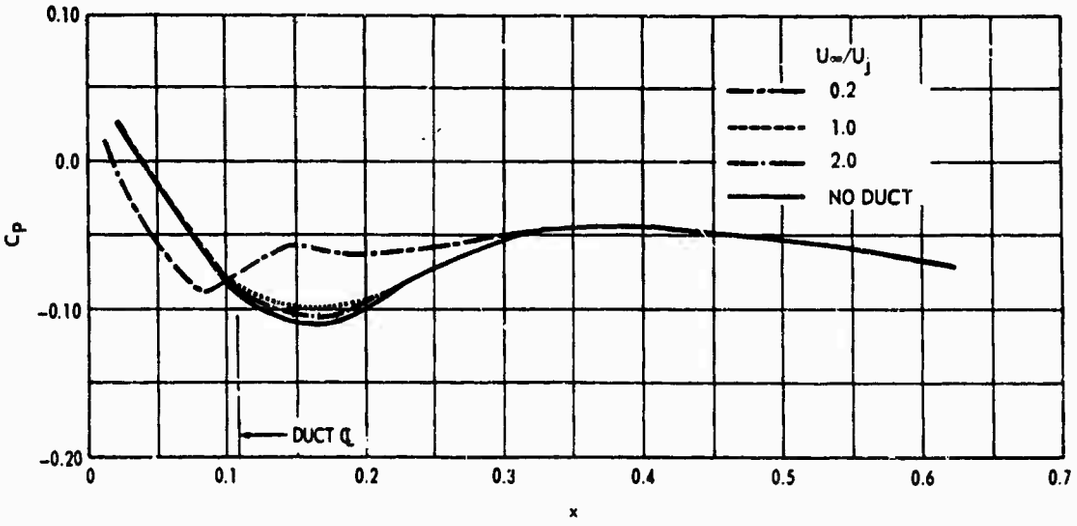

Figure 10 - Pressure Distribution off Body, Duct Entrance Flow for 4-Inch Duct at y = 0, z = 0.15

TABLE 1

Offsets for NSRDC Model 5166

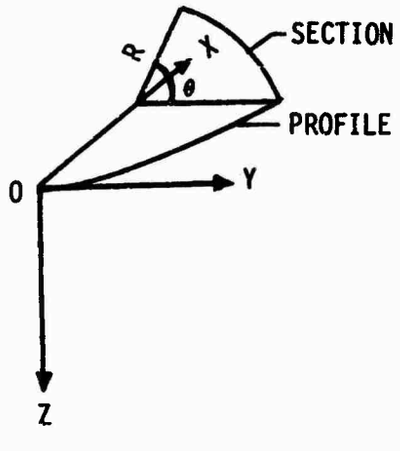

x	X in.	r	R in.
0.000	0.000	0.0000	0.000
0.002	0.320	0.0130	2.256
0.004	0.640	0.0184	3.184
0.007	1.280	0.0259	4.480
0.015	2.560	0.0362	6.269
0.026	4.480	0.0472	8.163
0.037	6.400	0.0555	9.600
0.055	9.600	0.0660	11.427
0.074	12.800	0.0740	12.800
0.092	16.000	0.0801	13.856
0.111	19.200	0.0848	14.662
0.129	22.400	0.0882	15.260
0.148	25.600	0.0906	15.677
0.185	32.000	0.0925	16.600
PMB	PMB		
0.578	100.00	0.0925	16.000
0.624	108.00	0.0910	15.750
0.671	116.00	0.0891	15.417
0.717	124.00	0.0857	14.833
0.763	132.00	0.0804	13.917
0.809	140.00	0.0730	12.625
0.855	148.00	0.0631	10.917
0.902	156.00	0.0486	8.417
0.948	164.00	0.0299	5.167
0.971	168.00	0.0183	3.167
0.994	172.00	0.0043	0.750
1.000	173.00	0.0000	0.000

WIND-TUNNEL EXPERIMENTS

TEST TECHNIQUE

A bow thruster is often designed to produce a specified force at zero ship speed. Therefore, flow experiments on ducts of different relative size, location, geometry, etc., for a given hull should be conducted at conditions that correspond to some equal force. It is assumed for t e present experiments that a bow thruster is designed for a total thrust T in a frictionless flow. For a straight-through duct, the force coefficient becomes ideally $\frac{T}{\rho A U_j^2} = 1.0$, from the jet reaction, and the relation of duct size to duct jet velocity for this value is

$$\frac{D}{D_1} = \frac{U_{j_1}}{U_j} \tag{1}$$

With the duct jet velocity selected to vary inversely with duct diameter, the velocity ratio U_∞/U_j was varied by changing the test speed in the wind tunnel. The choices of U_j and duct diameter (2 and 4 inches were the final choice) were based on consideration of duct Reynolds number, blower capacity for generating the duct flow, and compatibility with the range of operating speeds in the wind tunnel to cover the desired range of velocity ratio U_∞/U_j.

As a result of the described considerations, $30 \leq U_j \leq 160$ and $16 \leq U_\infty \leq 120$ (in feet per second) with the following minimum test Reynolds numbers:

$$R_{n_D} = 6.2 \times 10^4 \text{ for the duct}$$

$$R_{n_B} = 1.43 \times 10^6 \text{ for the hull}$$

Practically all test runs were made at a free-stream velocity U_∞ greater than 16 feet per second, which gives $R_{n_B} > 1.43 \times 10^6$. For both the 2- and 4-inch-diameter ducts, the experiments were conducted at duct Reynolds numbers safely higher than the critical value for turbulent pipe flow.*

*Note that at a given force, R_{n_D} does not change with duct size.

Average duct velocity U_j was determined from a pitot-static tube located on the duct axis. A value of 0.805 was used for the ratio of duct mean to maximum velocity. A correction of 0.976 was applied to approximate the true mean cosine component (axial velocity) for the duct turbulent flow.[10] Thus, U_j was obtained from the velocity head h and a coefficient c by

$$U_j = c\sqrt{2gh} = 0.786\sqrt{2gh}$$

The flow was visualized by smoke by a straightforward procedure which will not be discussed. Pressure distribution measurements were obtained from a straight-tube manometer board using alcohol as the metering fluid.

FLOW-VISUALIZATION RESULTS

Figures 11 through 13 respectively show the jet flow at various U_∞/U_j ratios for the 4-inch duct, the 2-inch duct, and the 2-inch duct with an extension. The progressive bending of the thruster jet in the downstream direction with increasing U_∞/U_j is evident. It is also obvious that the larger diameter duct produces a thicker jet outflow which covers more of the hull surface. This is an important factor in determining the magnitude of the interaction force when considered in connection with the pressure defect (discussed later). The manner in which the jet outflow "touches down" on the hull and the approximate value of U_∞/U_j at which this condition occurs are shown by the flow photographs. In particular, it is very noticeable that touch down is deferred to a higher U_∞/U_j and occurs further aft on the hull (Figure 13) when an extension is attached to the thruster duct.

PRESSURE DISTRIBUTION RESULTS

Much more quantitative knowledge of the jet outflow and its probable effects on the total interaction force can be gleaned from pressure measurements than can be inferred from flow visualization. Figures 14-16 show the separate pressure distributions for each configuration. Figures 17-19 give the pressure coefficient C_p cross faired against U_∞/U_j, with the hull axial coordinate x as parameter. As can be seen in Figures 14-16,

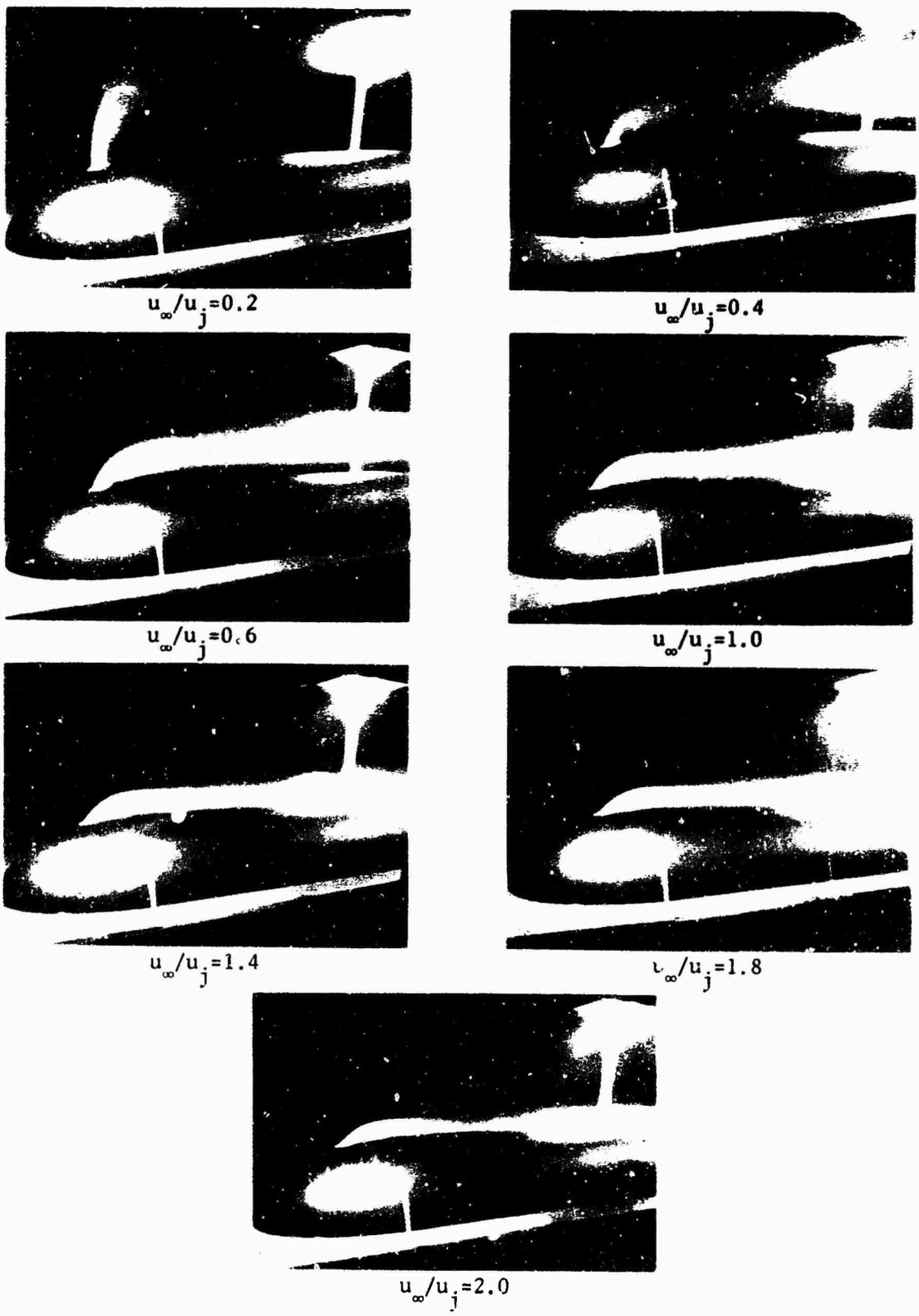

Figure 11 - Wind Tunnel Jet Flow, 4-Inch Duct

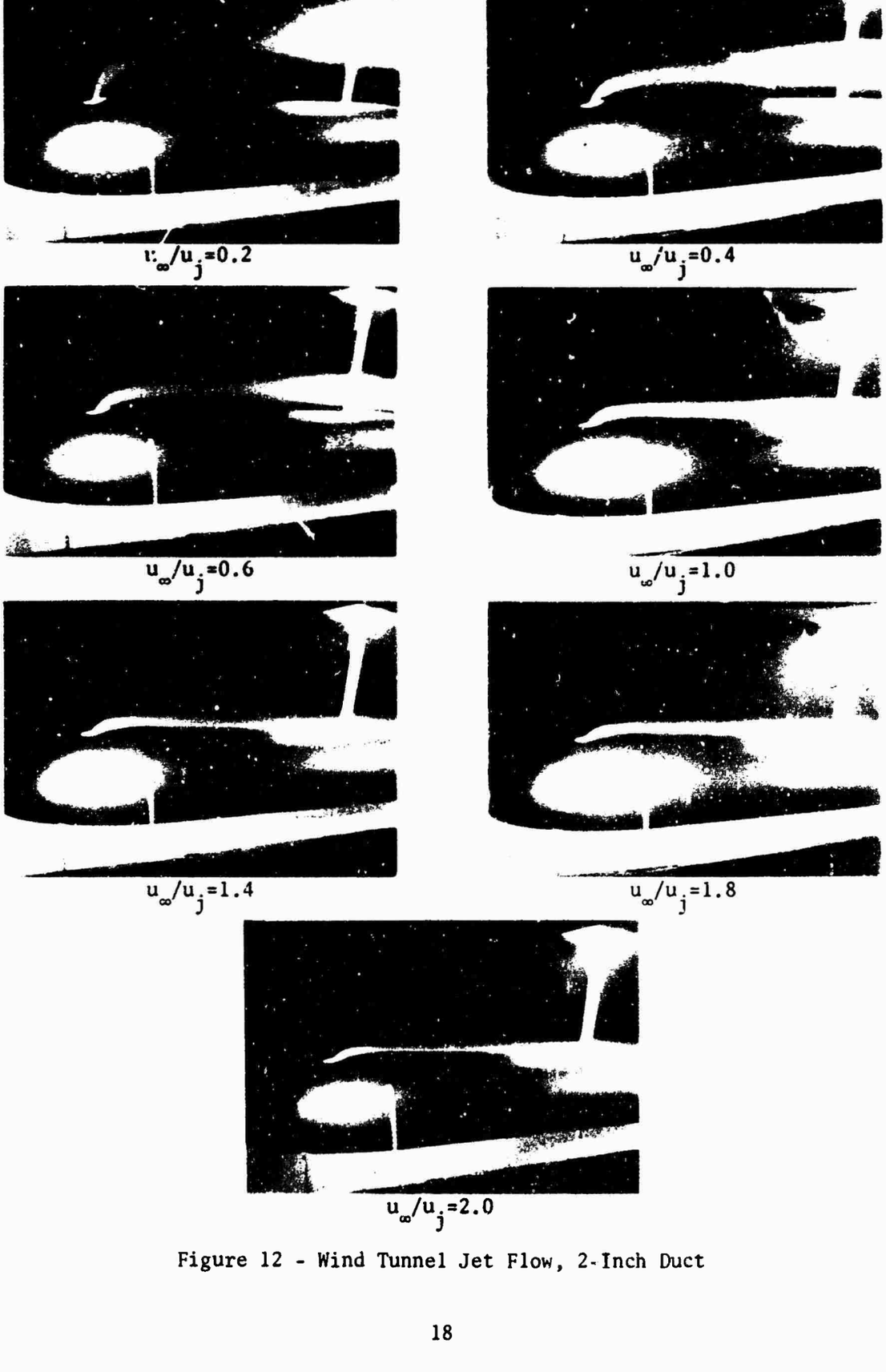

Figure 12 - Wind Tunnel Jet Flow, 2-Inch Duct

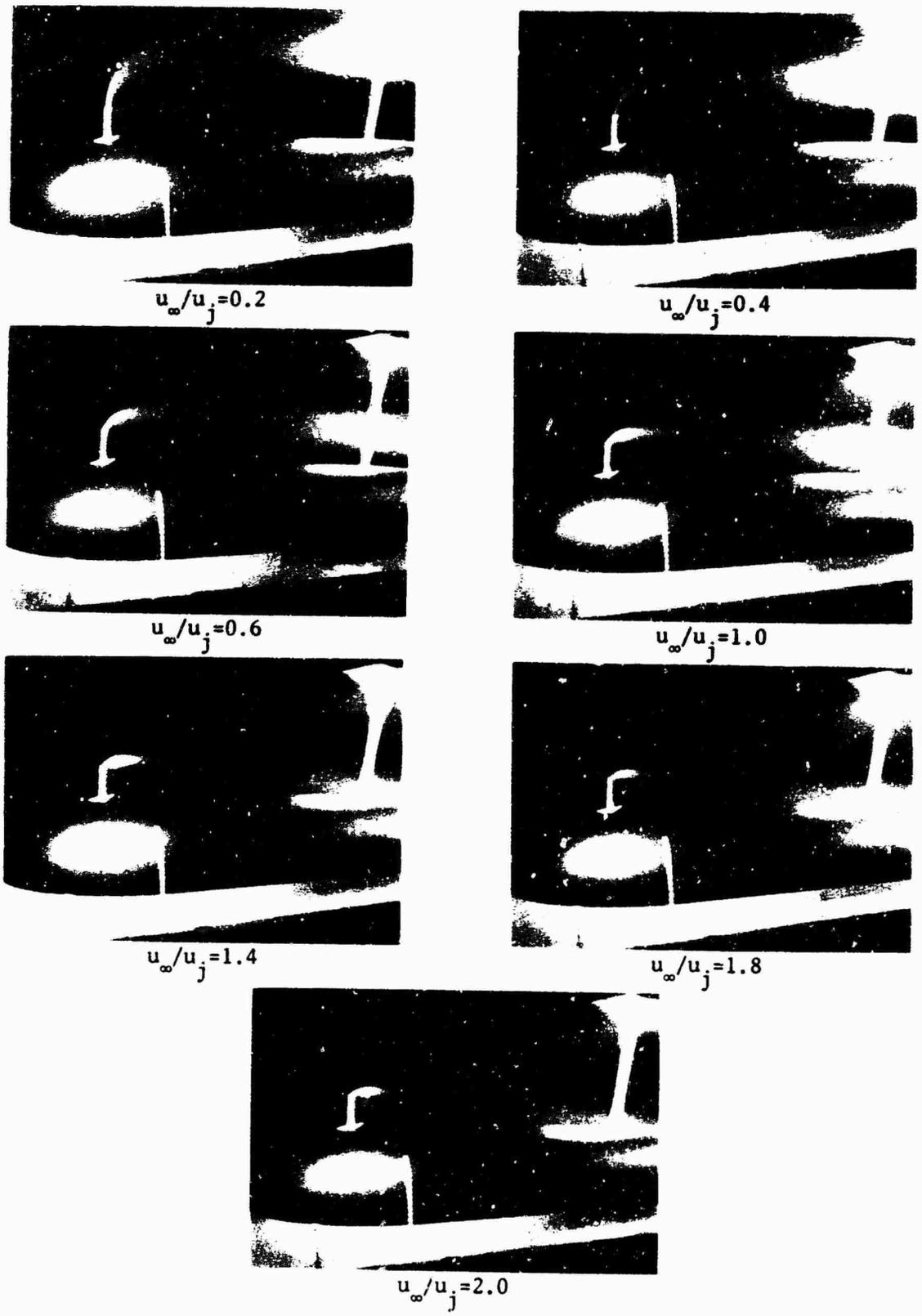

Figure 15 - Wind Tunnel Jet Flow, 2-Inch Duct with Extension

Figure 14 - Pressure Distribution Test Results for 4-Inch Duct

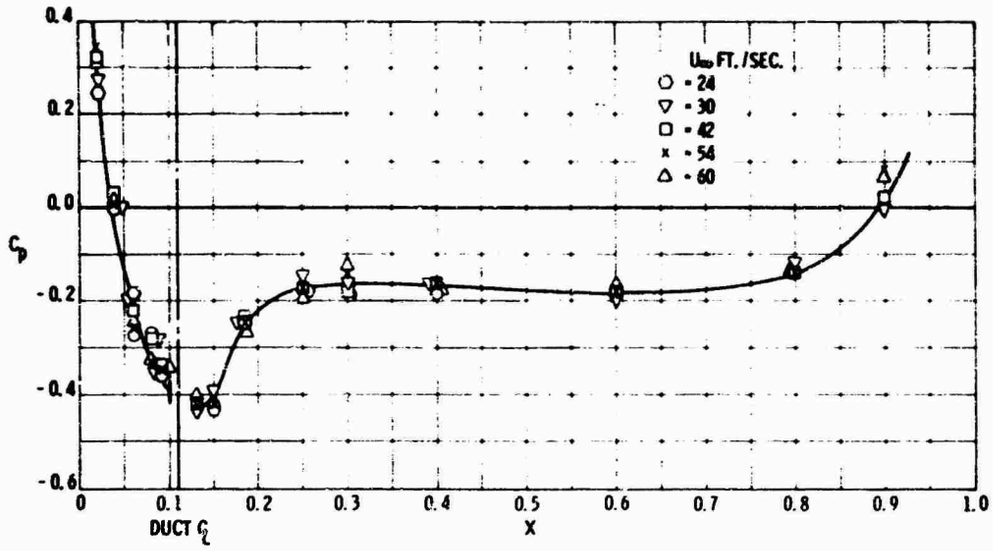

Figure 14a - At $U_j = 0.0$

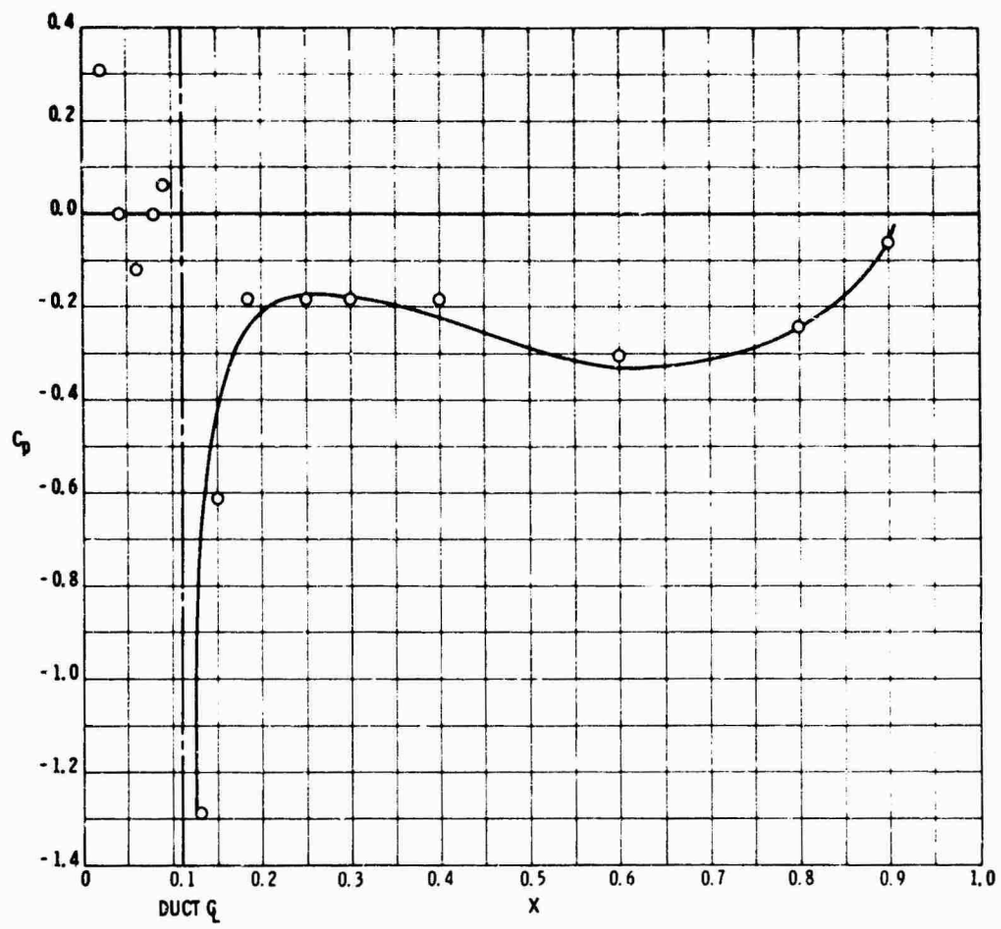

Figure 14b - At $U_\infty/U_j = 0.398$

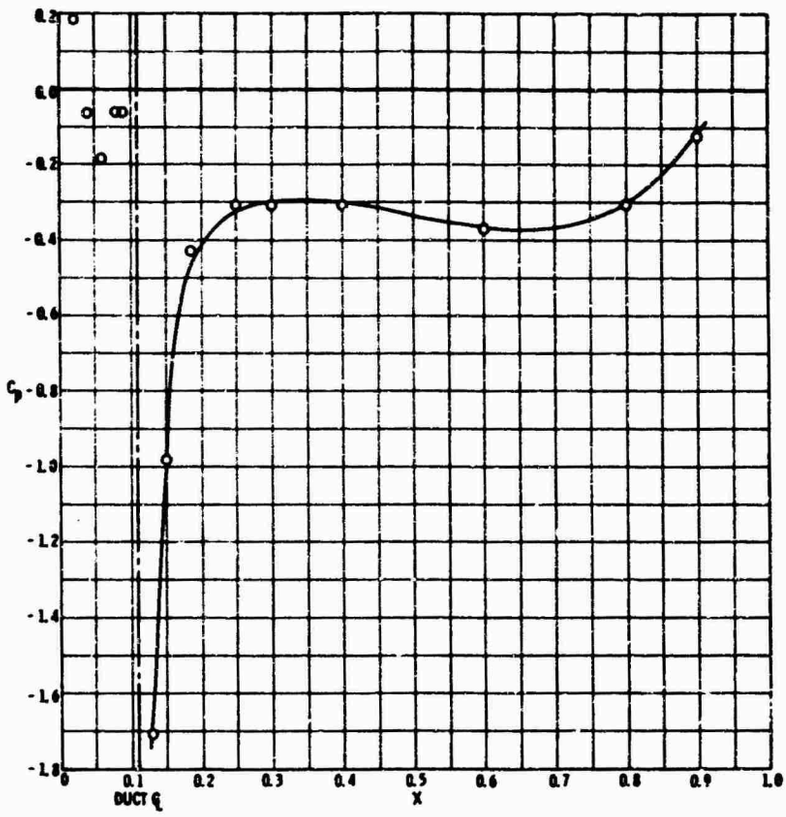

Figure 14c - At U_∞/U_j = 0.567

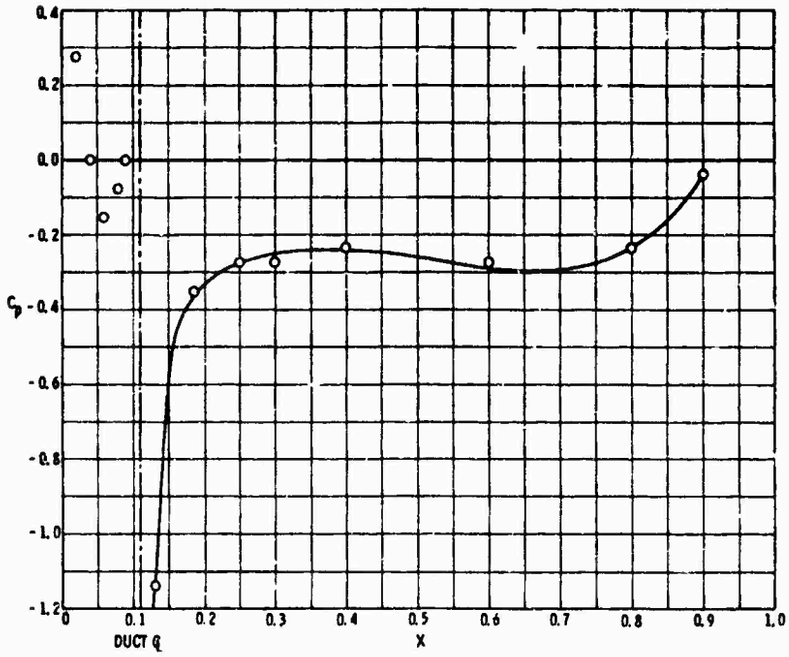

Figure 14d - At U_∞/U_j = 0.979

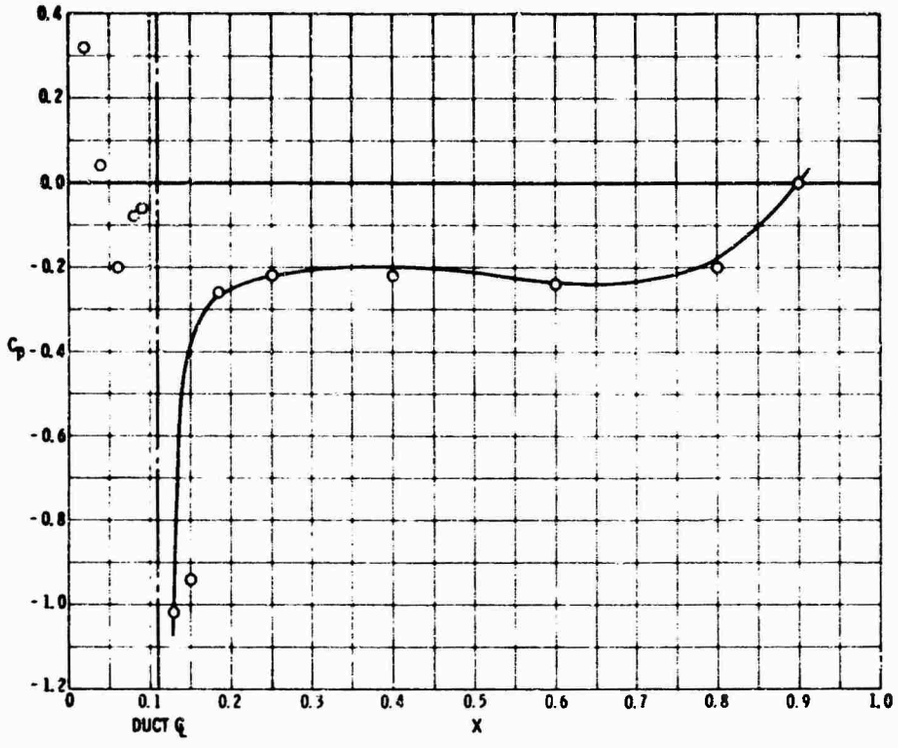

Figure 14e - At U_∞/U_j = 1.39

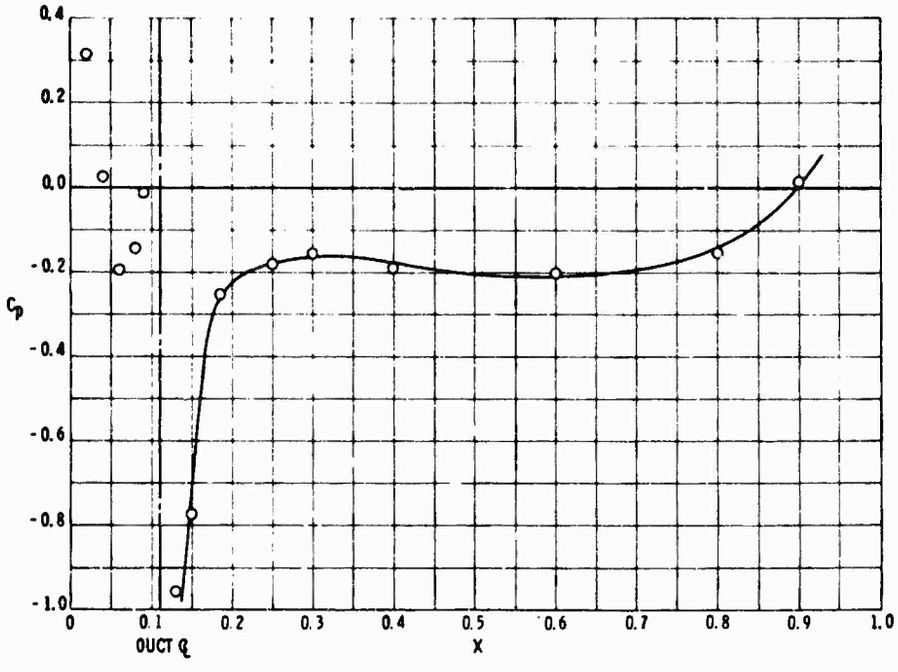

Figure 14f - At U_∞/U_j = 1.78

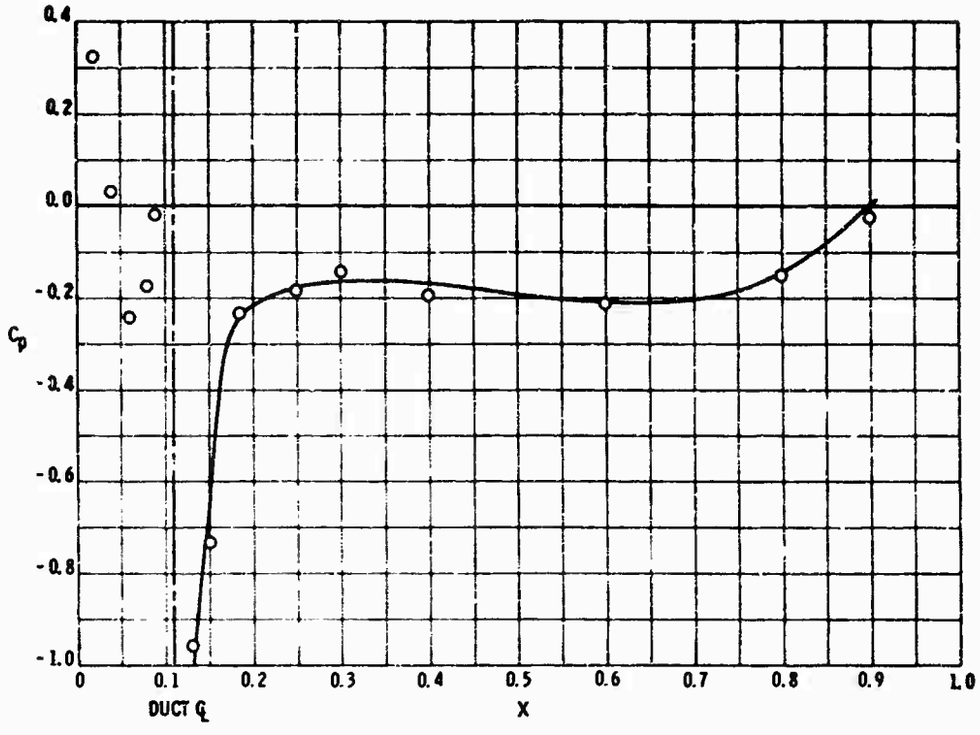

Figure 14g - At U_∞/U_j = 2.00

Figure 15 - Pressure Distribution Test Results for 2-Inch Duct

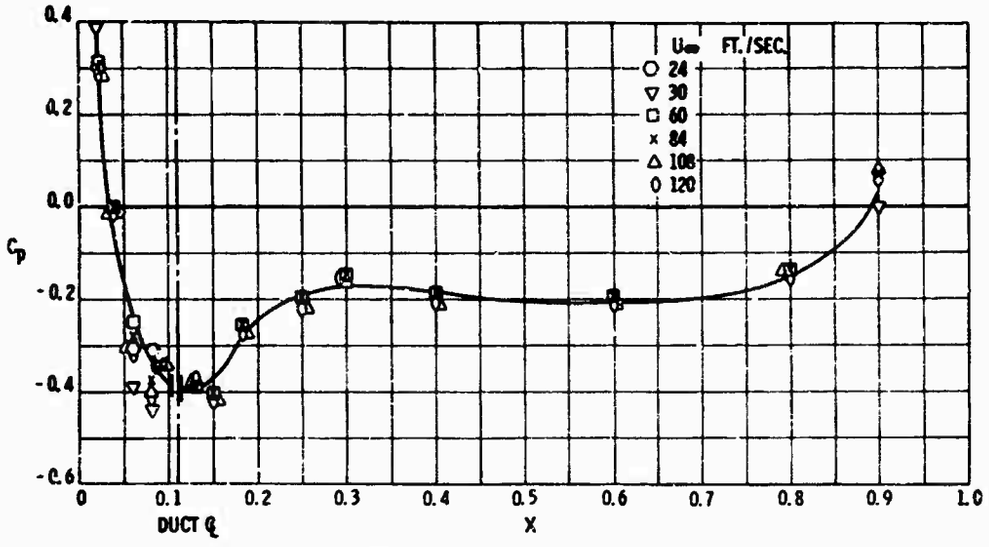

Figure 15a - At U_j = 0.0

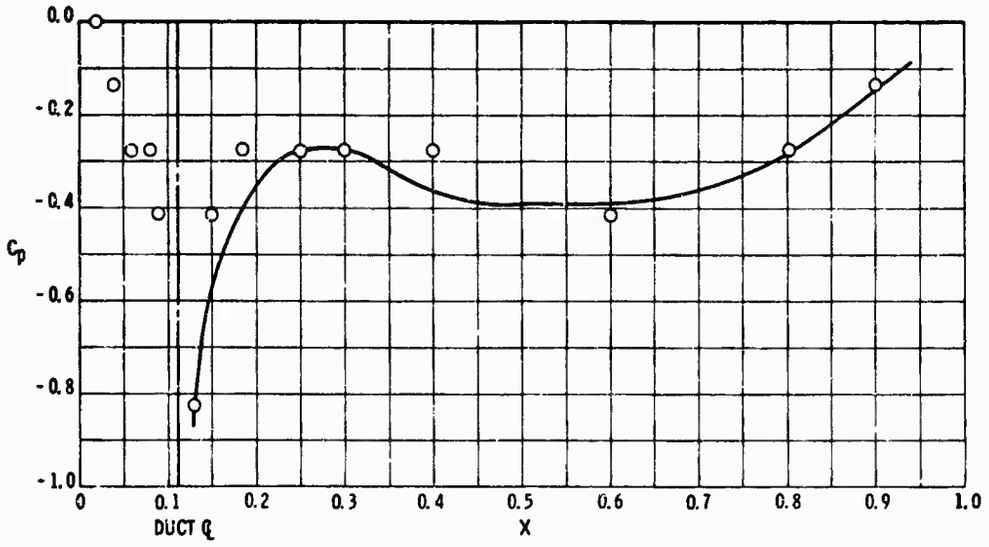

Figure 15b - At U_∞/U_j = 0.200

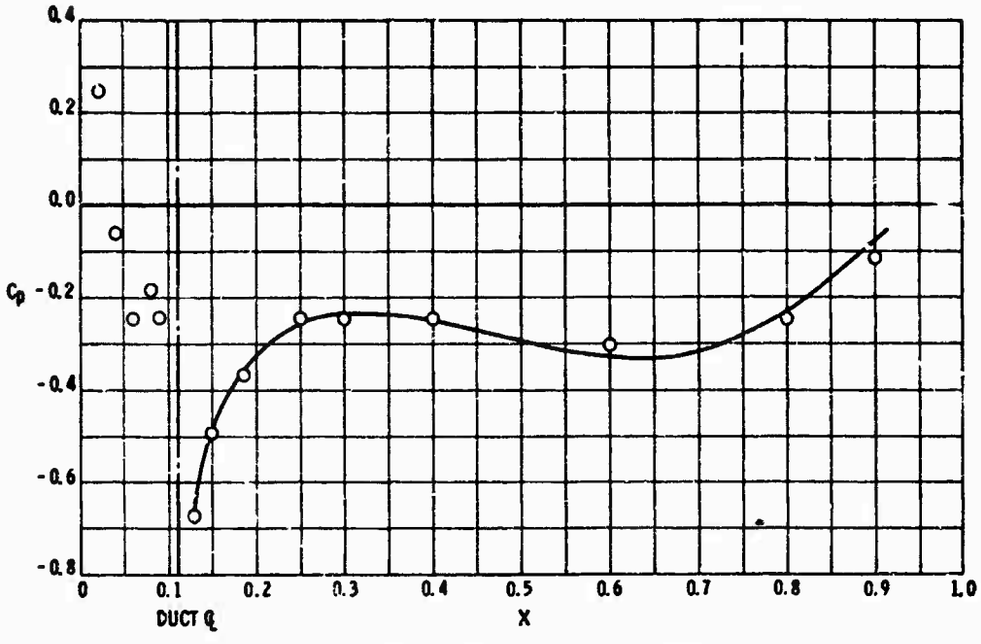

Figure 15c - At U_∞/U_j = 0.393

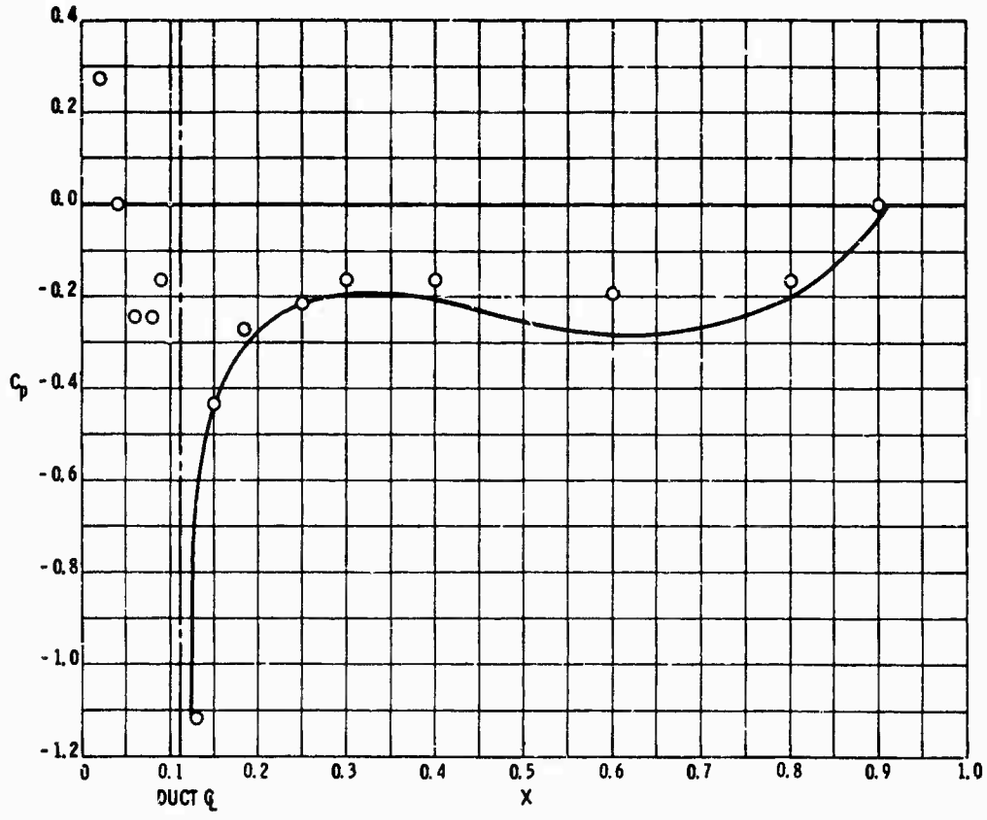

Figure 15d - At U_∞/U_j = 0.617

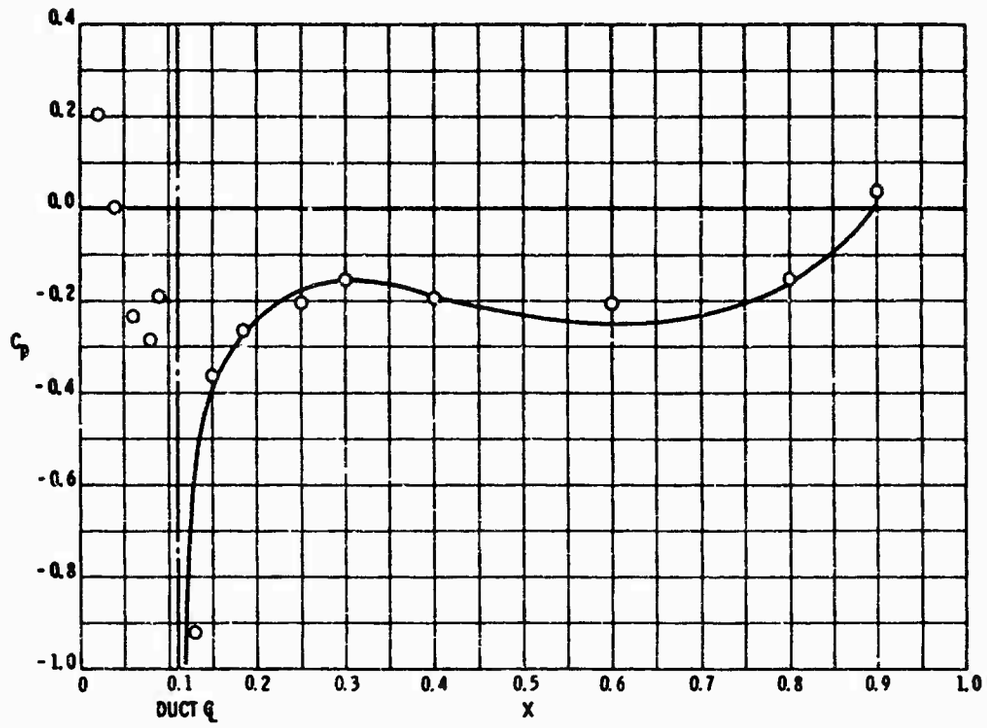

Figure 15e - At U_∞/U_j = 0.999

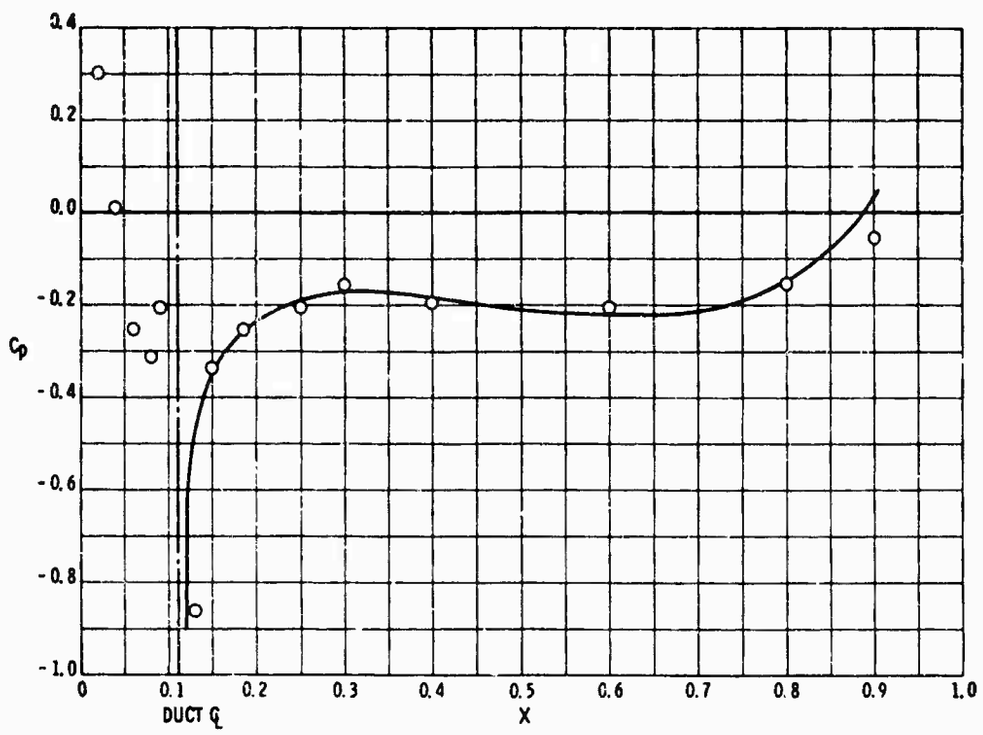

Figure 15f - At U_∞/U_j = 1.39

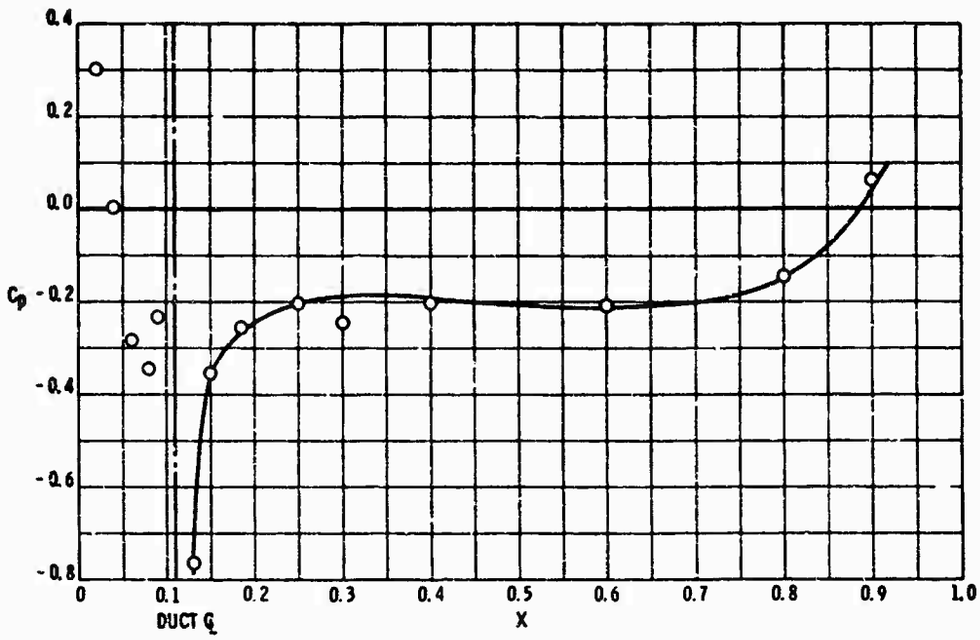

Figure 15g - At U_∞/U_j = 1.81

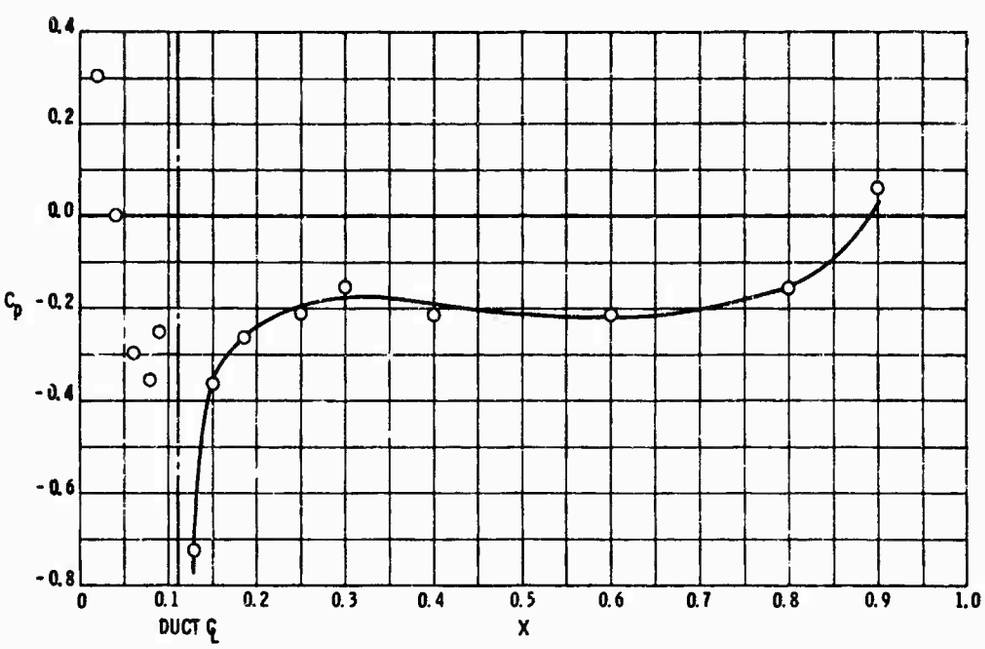

Figure 15h - At U_∞/U_j = 2.02

Figure 16 - Pressure Distribution Test Results for 2-Inch Duct with Extension

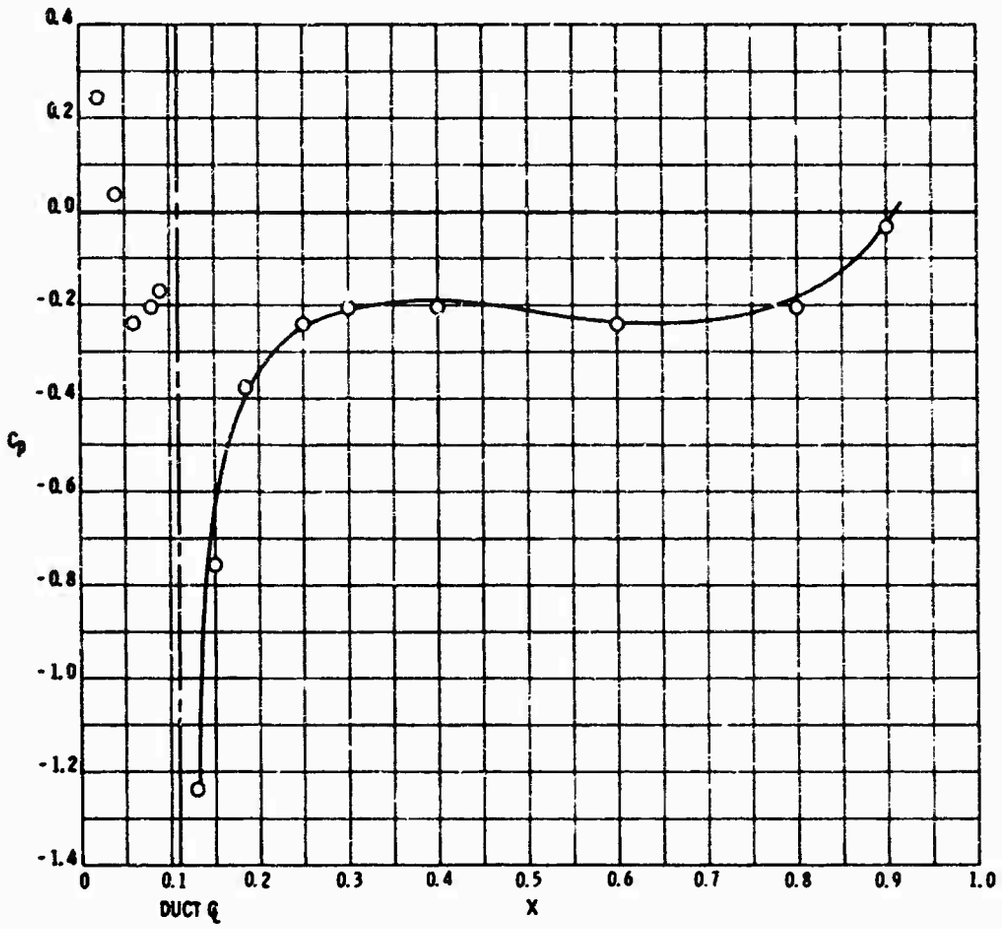

Figure 16a - At $U_\infty/U_j = 0.245$

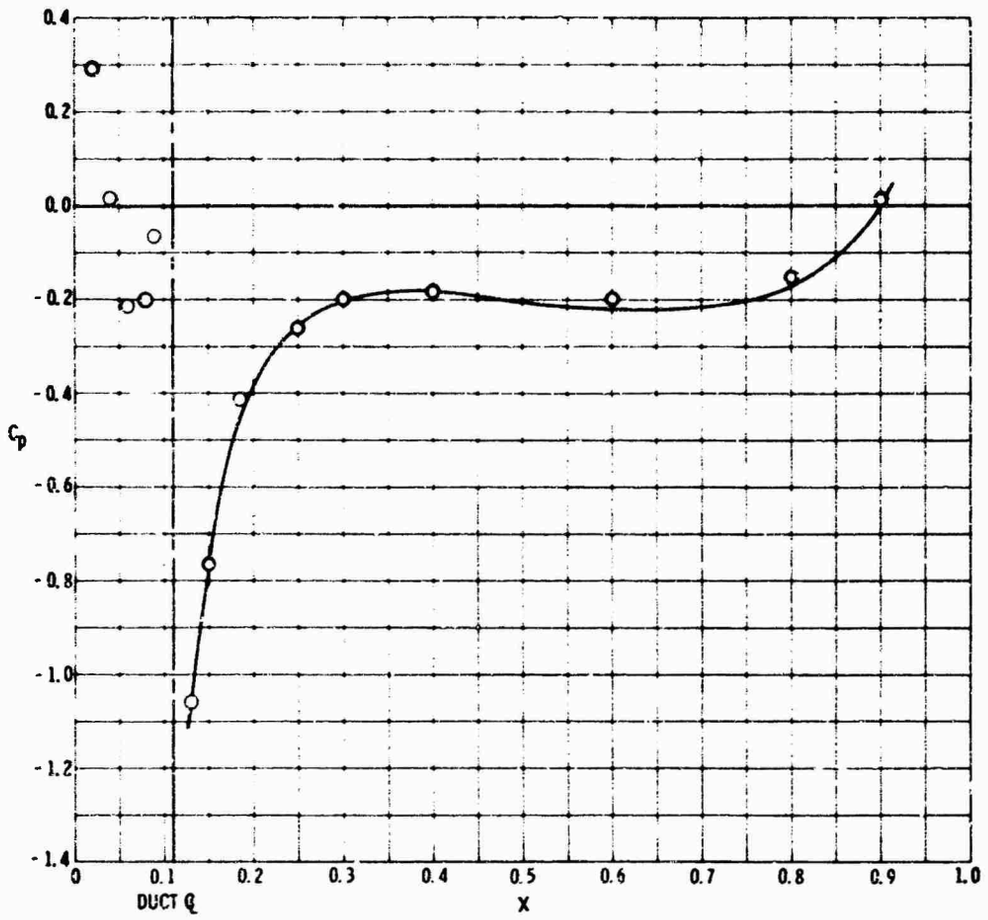

Figure 16b - At U_∞/U_j = 0.391

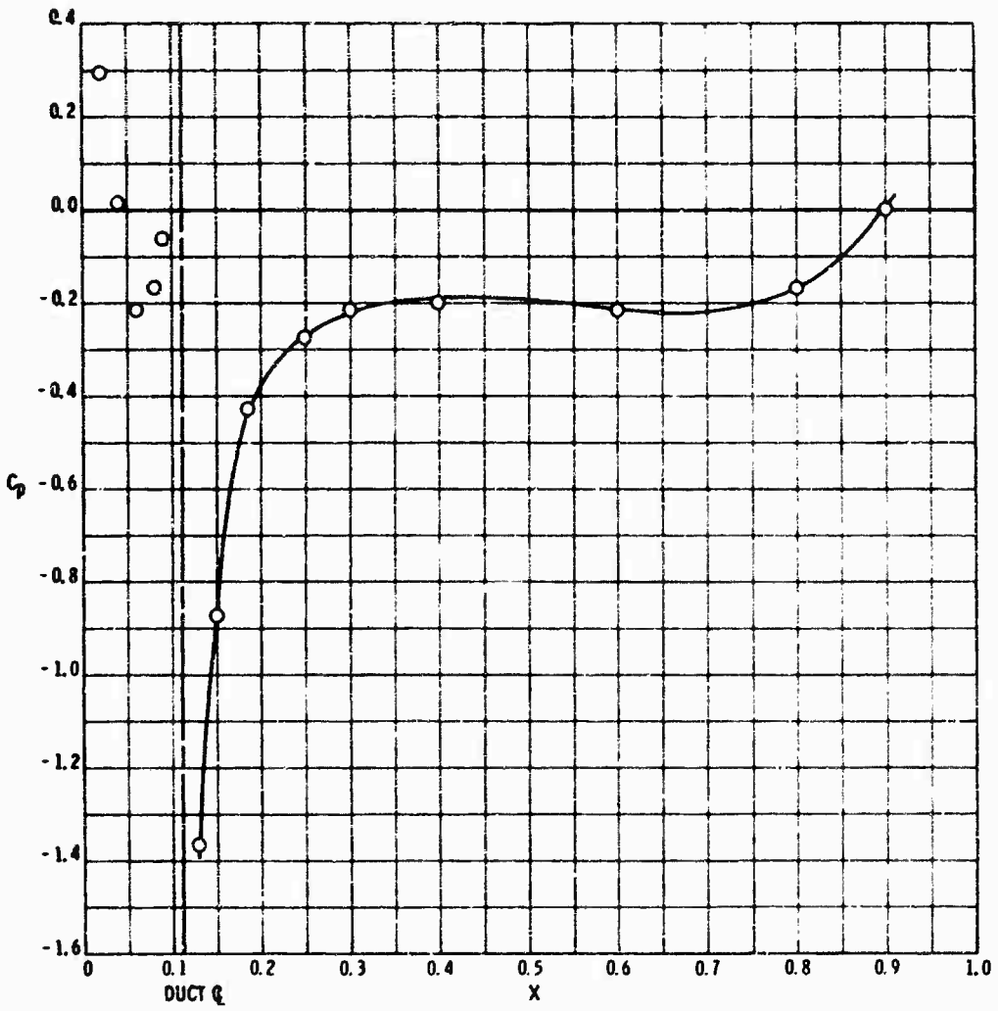

Figure 16c - At U_∞/U_j = 0.603

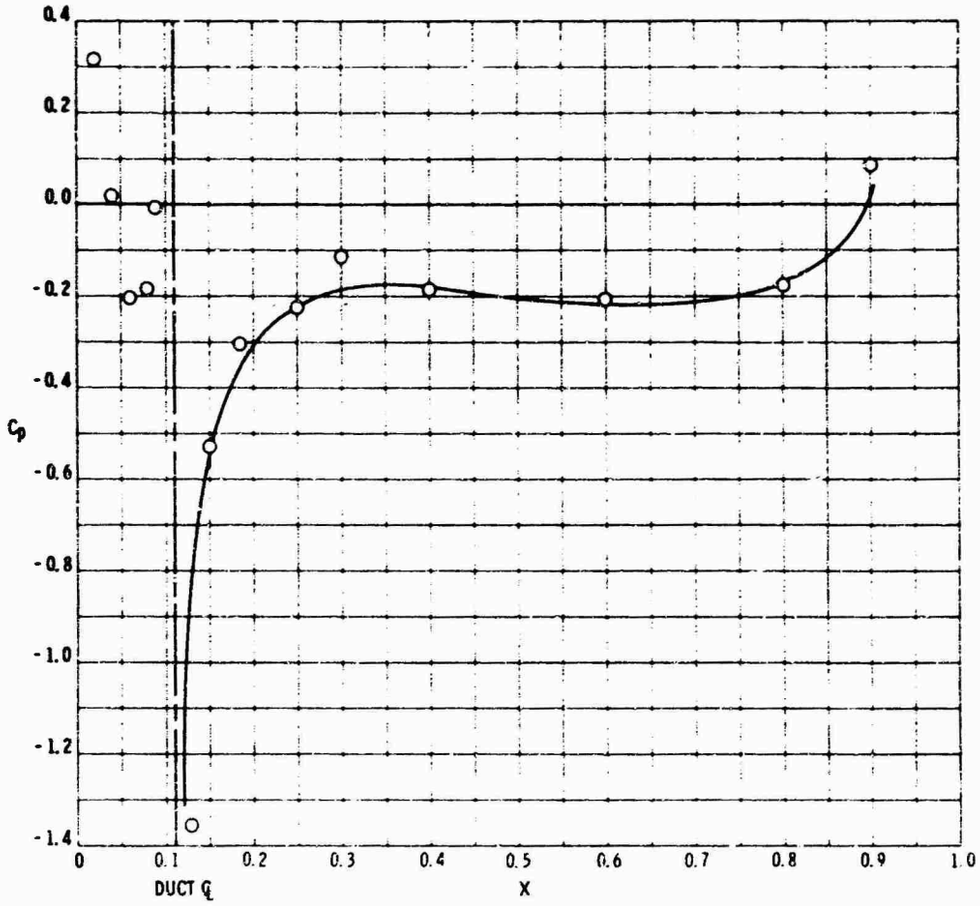

Figure 16d - At U_x/U_j = 0.985

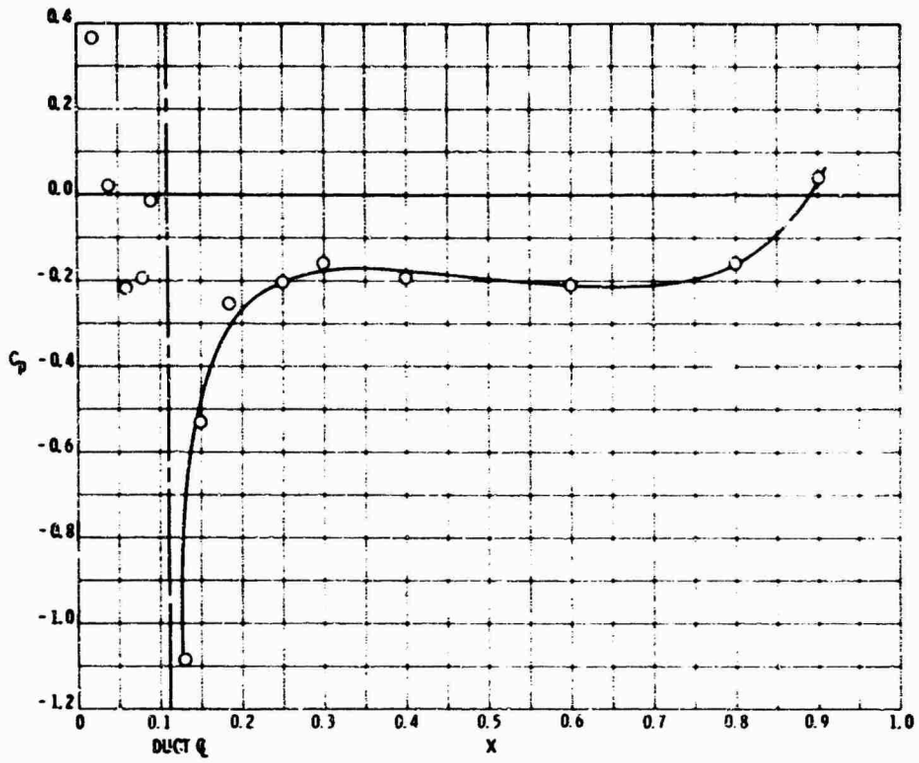

Figure 16e - At U_∞/U_j = 1.39

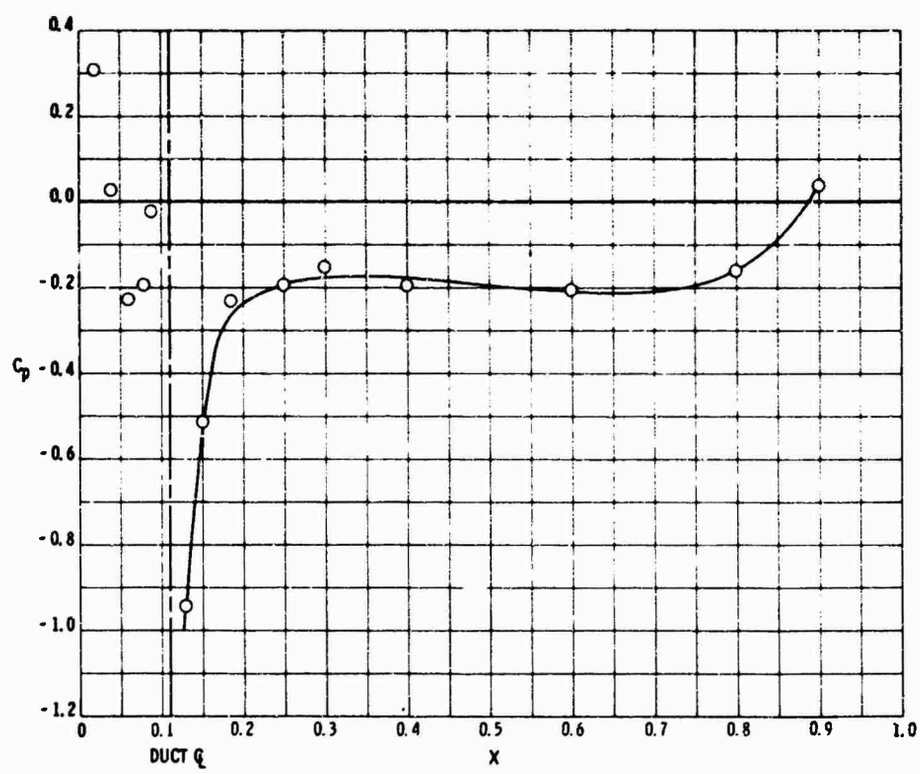

Figure 16f - At U_∞/U_j = 1.86

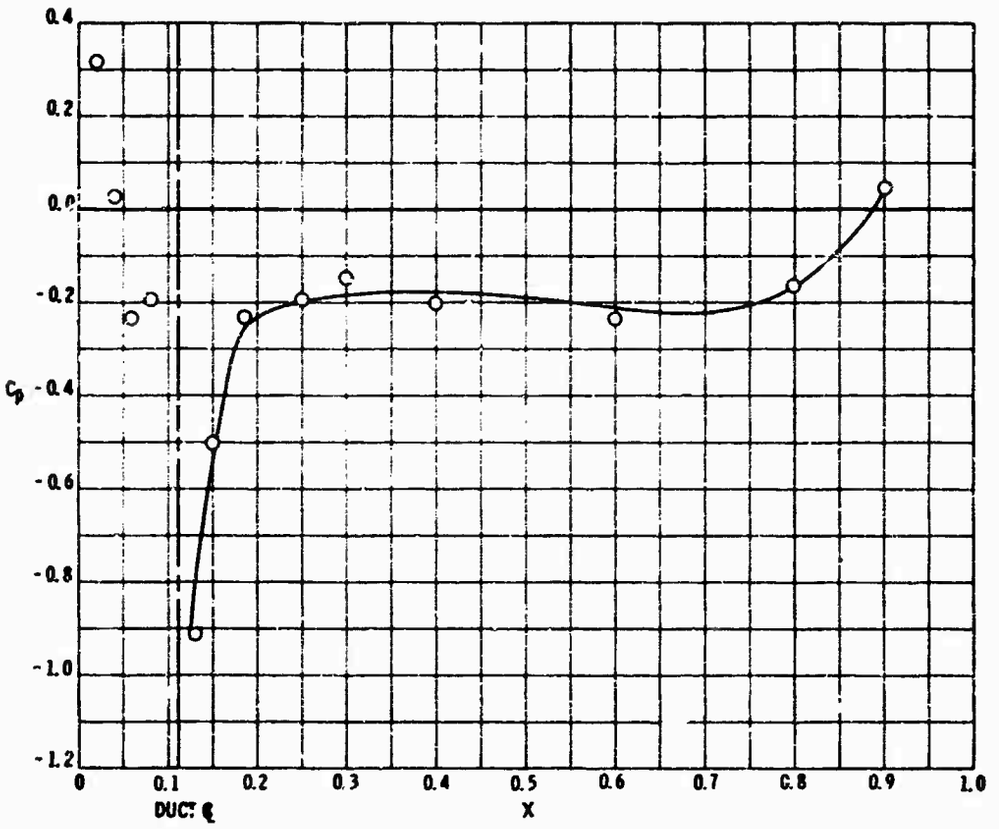

Figure 16g - At U_∞/U_j = 2.05

the cross-fairing process generally resulted in final faired curves that adhered closely to the data points shown. Figures 20-22 are composite graphs that give the pressure defect $\Delta C_p = (C_p)_{U_j} - (C_p)_{U_{j=0}}$ as a function of x, with U_∞/U_j as the parameter. A limited angular pressure survey (around hull girth in the duct centerplane) showed no duct outflow disturbance beyond 20 degrees from the top, port, and starboard except for velocity ratios $U_\infty/U_j < 0.5$. No disturbance was evident at 60 degrees for any outflow condition.

As can be seen in Figures 14-16, no attempt was made to draw curves through the data points ahead of the duct. These points of measurement are in a very steep pressure gradient and are not numerous enough to permit accurate fairing. Moreover, a pressure jump occurs across the duct opening. The data do show some retardation of the flow just ahead of the open-duct outflow. The flow forward of the 2-inch duct with the pipe extension would come to rest (stagnation point) at the pipe surface. This is indicated by the data points ahead of the pipe extension where a pronounced increase in C_p is evident.

The dependence of C_p on U_∞/U_j is shown in Figures 17-19. The variation indicated in Figure 17 for the 4-inch duct gives a distinct minimum C_p which occurs at $U_\infty/U_j \approx 0.6$ at all stations along the meridian profile. Thus, there is a critical value of the velocity ratio for this configuration whereas (as can be seen in Figure 18) this is not so for the 2-inch duct. A monotonic variation in C_p (less negative with increasing U_∞/U_j) is exhibited at each value of the parameter x. C_p is essentially independent of U_∞/U_j for the 2-inch duct with the extension; see Figure 19. Close behind the pipe extension, namely, x = 0.2, a flat suction peak ($C_p \approx -0.4$) occurs at a U_∞/U_j ratio of approximately 0.4. This is expected because of the high eddy flow immediately behind the pipe. One common feature for each plot of C_p versus U_∞/U_j is that C_p approaches a constant value at U_∞/U_j ratios greater than approximately 1.6.

The crux of the entire flow study is best demonstrated by an analysis of the pressure-defect ΔC_p curves presented in Figures 20-22. The pressure-defect ΔC_p is defined in this study as the difference between the pressure coefficient with outflow from the thruster duct and that for

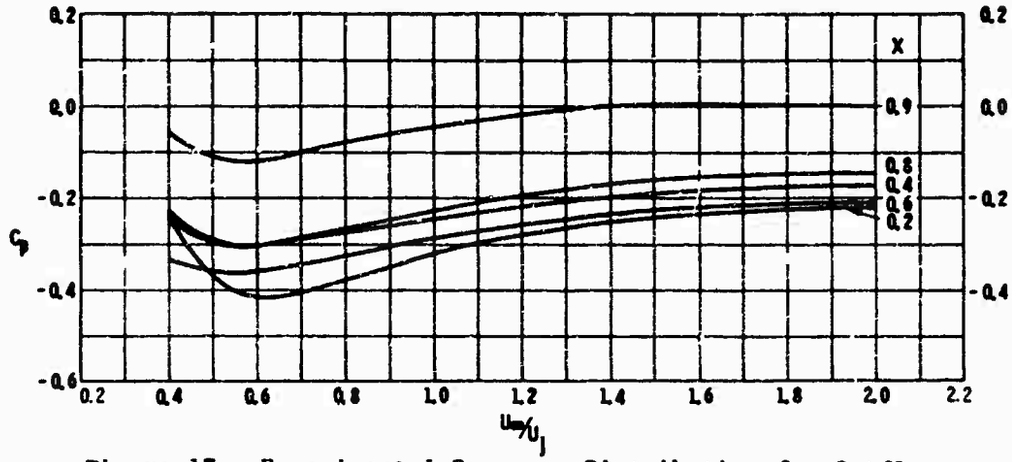

Figure 17 - Experimental Pressure Distribution for Outflow versus Velocity Ratic, 4-Inch Duct

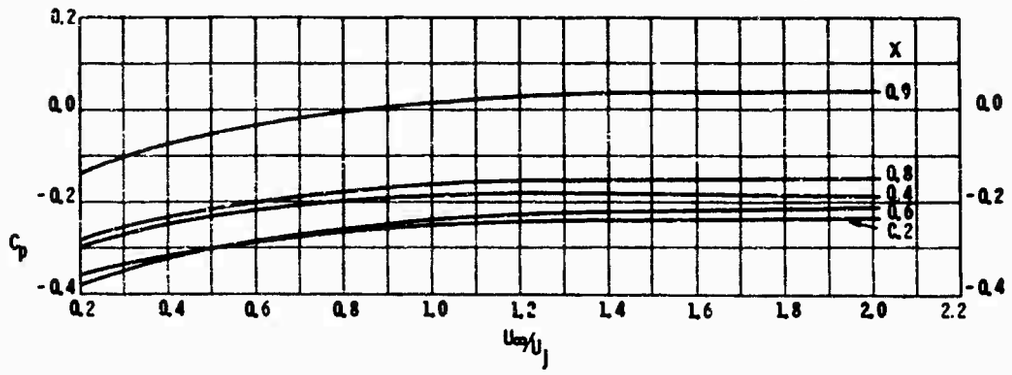

Figure 18 - Experimental Pressure Distribution for Outflow versus Velocity Ratio, 2-Inch Duct

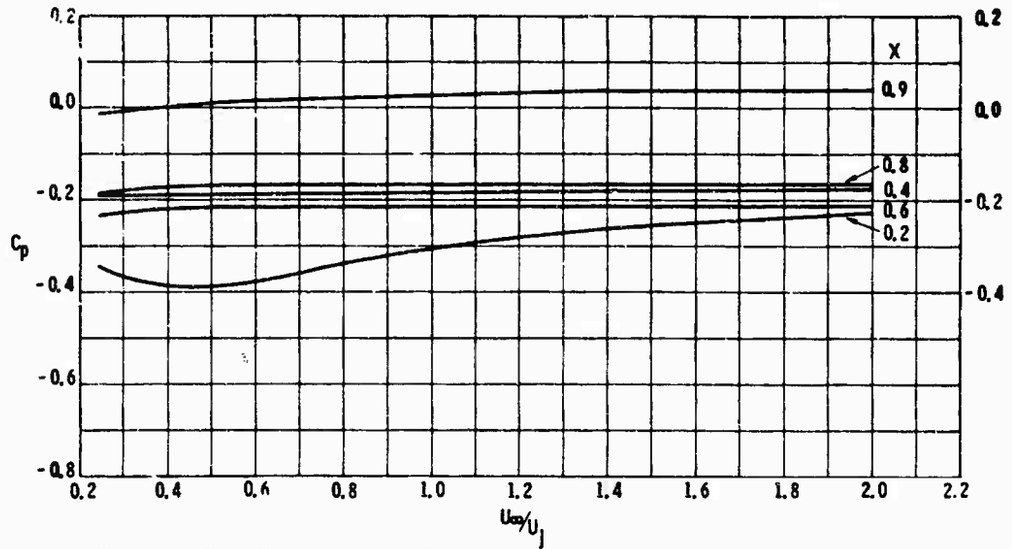

Figure 19 - Experimental Pressure Distribution for Outflow versus Velocity Ratio, 2-Inch Duct with Extension

no-duct outflow. For the case of the duct extension, the condition of no-duct outflow is with the extension removed. Continuing with reference to Figures 20-22, the generalized features that merit comment are:

1. The oscillatory nature of the curves with respect to x.

2. The large reduction in magnitude of ΔC_p for higher values of U_∞/U_j.

3. The effectiveness of the duct extension in reducing the pressure defect.

The last comment does not apply at positions x close behind the pipe extension because of the previously mentioned wake. However, the main concern is to verify a persistent outflow effect on the hull at large distances downstream. An index of hull surface lateral force and moment due to duct outflow can be obtained by integrating ΔC_p over an elementary lengthwise strip. Calculations for the 4-inch duct at $U_\infty/U_j = 0.4$ and 1.4 revealed that the center of action was well behind the thruster-duct axis. Although not considered, a component of the resultant surface force in the x-direction acts on the hull when $dr/dx \neq 0$. Since this x-force is asymmetrically applied with respect to the ship centerplane, an additional body-turning moment (likely to be small) is brought into play.

It is of interest to establish the three approximate flow regimes mentioned previously (PRINCIPAL CONSIDERATIONS) which plausibly describe the behavior of ducted bow thrusters in terms of the parameter U_∞/U_j. An approximate range can be tabulated from the flow photographs and the ΔC_p curves of Figures 20 and 21 as follows:

Flow Regime	U_∞/U_j for 2-Inch Duct	U_∞/U_j for 4-Inch Duct
1. Low	$<< 0.2$	< 0.2
2. Critical	≈ 0.2 to 0.4	≈ 0.4 to 0.6
3. High	> 0.6	> 1.0

From the viewpoint of interaction, Flow Regime 1 is of slight importance inasmuch as the body moment at low-ahead speed differs little from the static condition of thruster operation. However, something must be said about the important Regimes 2 and 3.

Up to this point, the experimental results have been examined in a general manner and in terms of nondimensional coefficients. It is logical

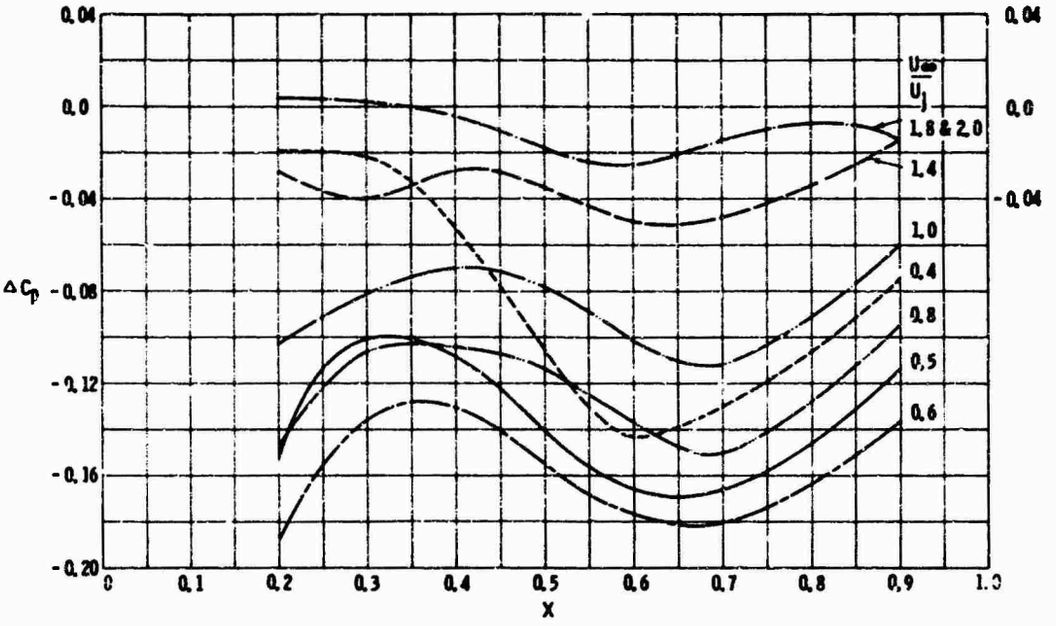

Figure 20 - Pressure Defect Associated with Outflow versus Longitudinal Position, 4-Inch Duct

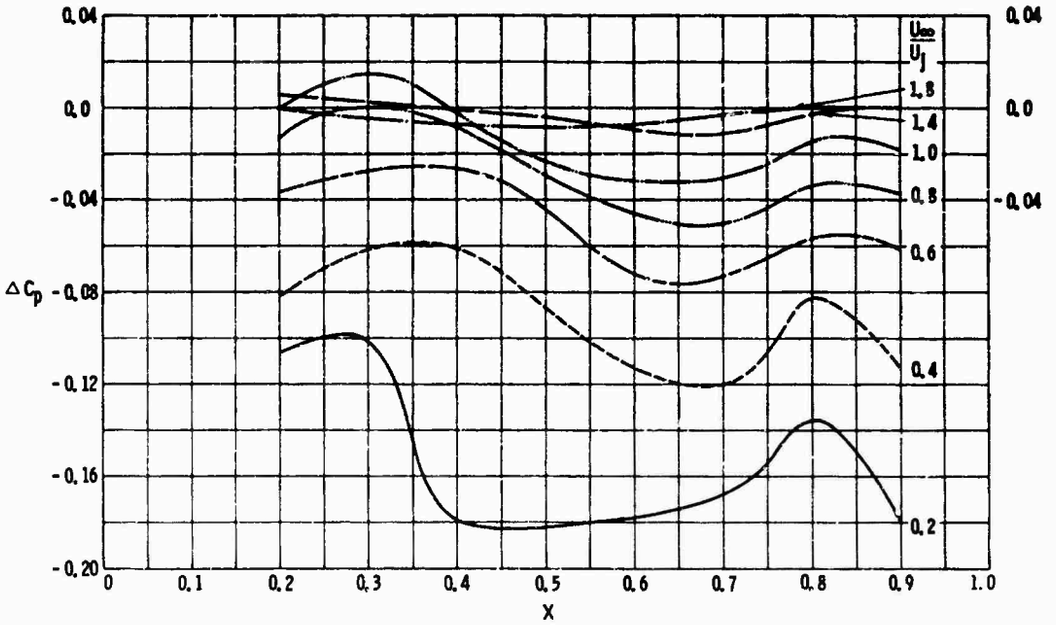

Figure 21 - Pressure Defect Associated with Outflow versus Longitudinal Position, 2-Inch Duct

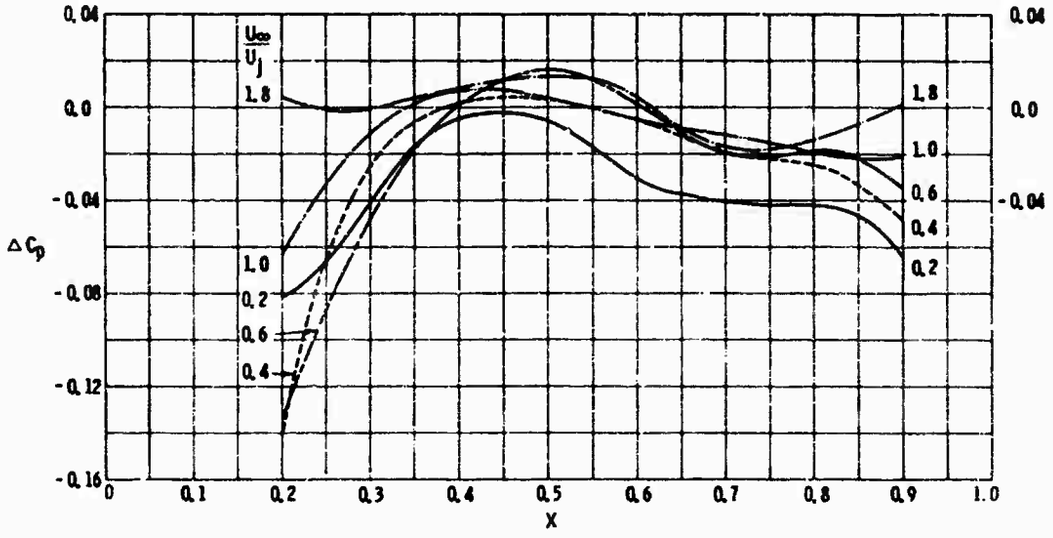

Figure 22 - Pressure Defect Associated with Outflow versus Longitudinal Position, 2-Inch Duct with Extension

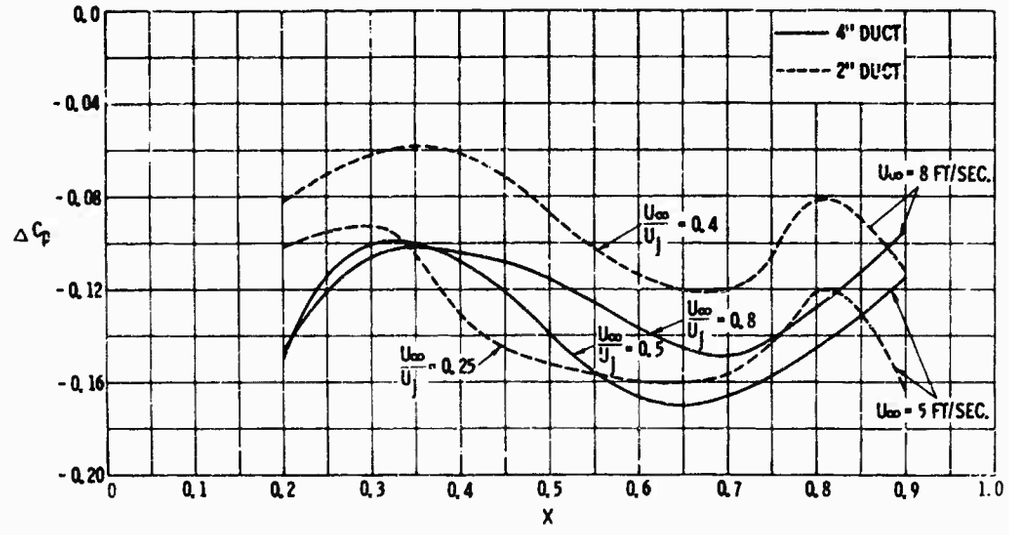

Figure 23 - Comparative Pressure Defects Associated with Outflow

to ask the following question, "What is the best thruster configuration and thruster operating condition, in a qualitative sense, for the subject hull within the scope of the present work?" To define what is best requires some constraint or assumption as to conditions. As indicated earlier, the flow tests were conducted at jet velocities that would ideally produce equal static force for different duct sizes. A practical approach seems to be a determination of the arrangement that gives the most favorable interaction on body moment for equal static force and for a prescribed ship speed. The comparative curves of pressure defect ΔC_p shown in Figure 23 were derived with this philosophy in mind. It is obvious that meaningful thruster comparisons must be made at unequal velocity ratios U_∞/U_j. The two selected ship speeds in Figure 23 provide a range of U_∞/U_j for the critical flow and marginally high flow regimes. At U_∞ = 5.0 feet per second, it can be seen that there is no significant difference in the pressure defect between the 2- and 4-inch ducts. At U_∞ = 8.0 feet per second, the 2-inch duct definitely has a smaller pressure defect than does the 4-inch duct. This fact coupled with the thicker jet outflow of the 4-inch duct, which covers more hull surface, leaves no doubt as to the superiority of the 2-inch duct with regard to the interaction force. However, propeller efficiency must be considered in the total design problem. Reference 1 suggests that from the viewpoint of interaction, it might be beneficial to use a large-diameter, low-velocity (soft) jet for higher ship speeds. The present result seems contrary; however, the terms large, small, etc., are quite relative. In the final analysis, it may be better to design a bow thruster for maximum efficiency at the static condition and then to control the outflow by some mechanical means such as a retractable extension, internal deflecting vanes, etc., thereby obtaining a pressure defect that is relatively insensitive to the ratio U_∞/U_j.

ANALYSIS FOR JET OUTFLOW

It is desirable to find a phenomenological expression that could be used to collapse the pressure-defect curves of Figures 20 and 21. This would permit a single equation to be used for interpolation and for

generalization of the results with respect to duct size. A method similar to that used to determine pump-flow characteristics was found to give reasonable results. Bow-thruster outflow can be characterized independently from the pumping device. That is to say, coefficients can be formed in terms of the jet velocity instead of the frequency of revolution of an impeller. This approach is particularly useful since bow-thruster flow can be generated by several means.

A pressure coefficient $\Delta C_p'$ and a flow coefficient ϕ are defined as

$$\Delta C_p' = \frac{\Delta p}{q_j} = \Delta C_p \left(\frac{U_\infty}{U_j} \right)^2$$

and

$$\phi = \frac{\forall}{B^2 U_\infty} = \frac{A U_j}{B^2 U_\infty}$$

where ΔC_p is equal to $(C_p)_{U_j} - (C_p)_{U_{j=0}}$ as previously defined,

$q_j = (1/2)\rho U_j^2$ is the jet dynamic pressure,

$\forall$ is the volume flow rate through the duct, and

B is the maximum beam of the hull.

The flow coefficient ϕ is a numeric which expresses the duct flow as a fraction of a pseudodisplacement flow around the hull. Consider the coefficient

$$\left(\Delta C_p'\right)\phi = \frac{(\Delta P)A}{\frac{1}{2}\rho B^2 U_\infty U_j} = \frac{A\left(\Delta C_p\right)}{B^2 \tan\theta}$$

where, as sketched, U_∞ 

$U_j/U_\infty = \tan\theta$ or $U_j\, U_\infty = U_\infty^2 \tan\theta$.

Thus it is seen that physically $\left(\Delta C_p'\right)\phi$ is a coefficient reflecting pressure change, duct size relative to ship beam, and first order bending of the jet outflow.

Mean values of the function ΔC_p versus x were calculated to generalize the curves of Figures 20 and 21. The data were used to calculate the product $\left(\Delta C_p'\right)\phi$ versus ϕ with the ratio of duct diameter to hull length D/L as a parameter. The results are plotted in Figure 24. The variation in the pressure-coefficient curves with x in Figures 20 and 21 was decreased by using the function $\left(\Delta C_p'\right)\phi$ because of the use of the flow angle θ. The assumption of no change with x means that $\Delta C_p'$ becomes a constant in an integration to obtain the center of action of hull-surface forces, but the center of action of the force is strongly dependent on jet diffusion over the hull-surface area.

A sine function is suggested by the shape of the curves of Figure 24. For no-duct outflow $\left(\Delta C_p'\right)\phi$ is zero; at some higher value of ϕ, the coefficient $\left(\Delta C_p'\right)\phi$ again becomes zero, corresponding to a relatively low value of velocity ratio U_∞/U_j where the thruster jet issues approximately perpendicular to the mainstream (static case). Within this interval, an equation of the form

$$\left(\Delta C_p'\right)\phi = a \sin (x + B)$$

is assumed with $x = n\phi$, $a = f$ (D/L) amplitude, $n = g$ (D/L) period, and B = 0 phase. A numerical evaluation of the constants results in the following final equation:

$$10^2 \left(\Delta C_p'\right)\phi = (-9.052\ D/L + 0.091) \sin [(-6830\ D/L + 244.5)\phi] \qquad (2)$$

In Equation (2), the choice of hull length L to nondimensionalize duct diameter was made (a) because for a given thruster size, ship turning rate depends on hull length and (b) because of the generally good agreement of flat-plate theory in this regard. The dashed lines of Figure 24 are the calculated curves; they include an interpolated curve for D/L = 0.0173 which corresponds to a 3-inch-diameter duct for NSRDC Model 5166. These curves should be faired with zero slope at the high-flow rate end.

Equation (2) is independent of scale, that is, the pressure $\Delta C_p'$ and flow coefficient ϕ were obtained from tests that were conducted at Reynolds numbers safely greater than the critical value for turbulent flow (see TEST TECHNIQUE). Equation (2) may be used to estimate bow-thruster

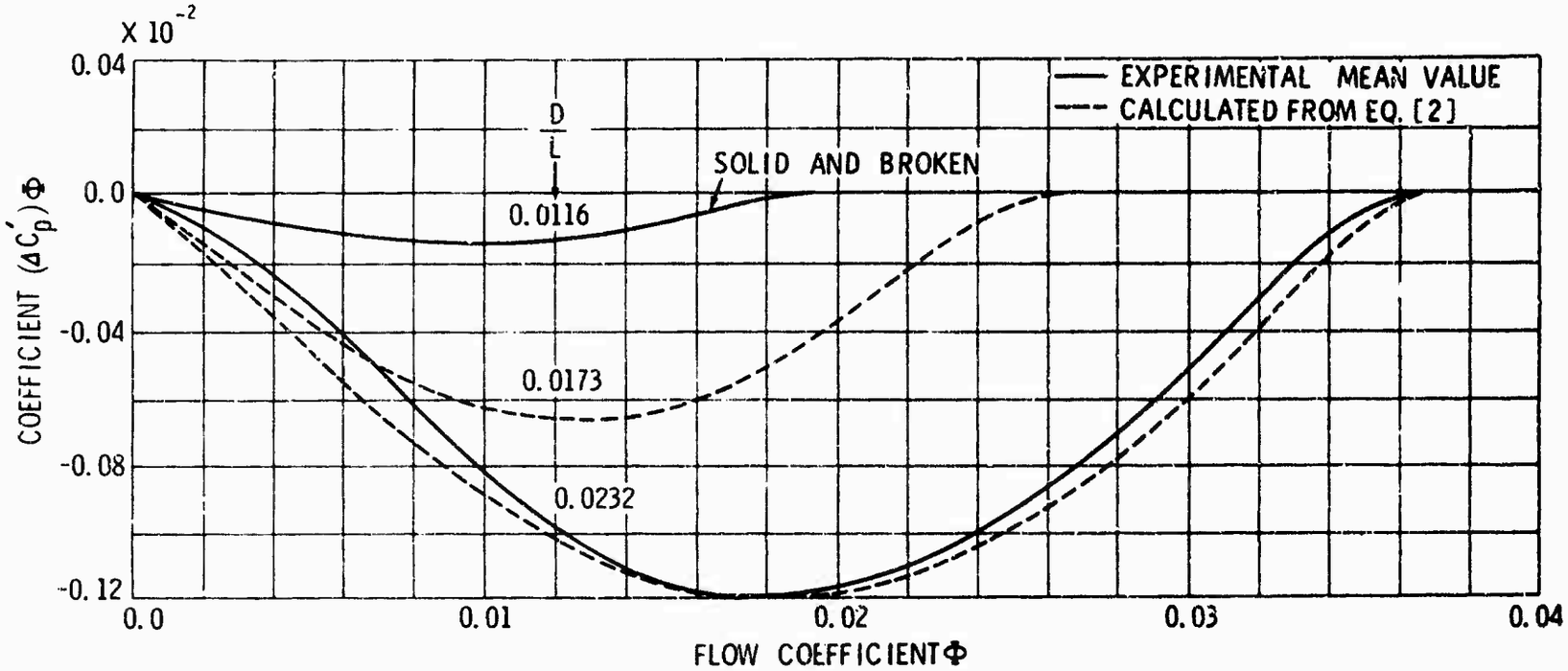

Figure 24 - Generalized Outflow Characteristics

outflow interaction for a prototype based on comparative pressure defect. Flow coefficients are used that correspond either to prescribed values or to a desired range of velocity ratio U_∞/U_j and duct size. An elementary hull force, hull moment, and center of action of the force can also be derived by using the calculated pressure coefficient $\Delta C_p'$. The incremental surface force per unit width is

$$\frac{\Delta F_s}{\ell} = (\Delta P \, dS) \frac{dx}{dS} \tag{3}$$

where ℓ is in the circumferential direction and S is a length along the body profile. The nondimensional surface force, moment, and center of action are, respectively,

$$C_{F_s} = F_s/L\ell q_j = \int_{x=a}^{b} \left(\Delta C_p'\right) dx \tag{4}$$

$$C_{M_s} = M_s/L^2\ell q_j = \int_{x=a}^{b} \left(\Delta C_p'\right) x \, dx \text{ and} \tag{5}$$

$$\bar{x} = \bar{X}/L = C_{M_s}/C_{F_s} \tag{6}$$

Equations (4) and (5) give an index of the surface force and moment and do not consider jet diffusion over the hull surface. In many cases, this would not seriously impair the usefulness of the data. In the case of the comparison between the two ducts discussed earlier (see PRESSURE DISTRIBUTION RESULTS), the smaller duct has less pressure defect and this, coupled with the wider jet outflow of the larger duct, left no doubt that the smaller diameter duct would produce a lower interaction force. Working back to ΔC_p by use of either the calculated or experimental curves of Figure 24 revealed that the smaller duct remained the proper choice.

Equation (2) can be used to estimate ΔP until more experimental data become available. The usual word of caution concerning the use of

empirical data applies in this case: the accuracy for extrapolation purposes is unknown; therefore, the use of Equation (2) should be limited to interpolation or reasonable extrapolation.

SUMMARY

It has been clearly demonstrated that the outflow effect (suction) on the hull persists to large distances downstream. This implies the use of a full-length vehicle to perform a definitive bow-thruster flow study at ahead speed. Although perhaps not fully recognized previously, the actual strength of the outflow low-pressure region is drastically reduced at higher ratios of U_∞/U_j, and this fact alone would result in a reduction of interaction forces. At the same time, the center of action of suction forces is probably shifted further aft due to jet diffusion and produces a more favorable turning moment at large U_∞/U_j ratios. The latter effect would be more important for hulls with either a long parallel middle body or full sections extending well aft. Steady turning with a bow thruster has not been considered in this investigation; however, model tests by Norrby[2] showed an increase in the turning moment from a bow thruster when the ship had a drift angle. The result seems plausible when viewed from the standpoint that this is equivalent to turning the duct slightly upstream.

Certain design implications for bow thrusters can be stated on the basis of both the present flow analysis and results presented elsewhere in the literature.

1. Performance of a bow-thruster propeller is hardly affected by vehicle ahead speed.[3,4]

2. Development of body-surface forces and moments due to duct-entrance flow at various ratios of U_∞/U_j is quite localized. This is in contrast to the important and extensive interaction between the main stream and the duct outflow.

3. The "tradeoff" on duct size should be considered in terms of installation adaptation and cost, thruster static efficiency (merit coefficient), and avoidance of the critical range of U_∞/U_j for vehicles with ahead-speed thruster-control requirements.[1]

4. The possibility of bow-thruster air drawing should be considered.

5. Developmental studies should be done for a specific thruster installation, particularly with regard to controlled deflection of jet outflow at ahead speed.[1]

A phenomenological analysis of duct outflow led to the following equation:

$$10^2\left(\Delta C_p'\right)_\phi = \left(-9.052\,\frac{D}{L} + 0.091\right)\sin\left[\left(-6830\,\frac{D}{L} + 244.5\right)\phi\right]$$

which is considered independent of absolute scale and can be used to estimate hull-pressure defect and elementary surface forces and surface moments for any prototype as a function of the ratio D/L and flow coefficient ϕ.

CONCLUSIONS

Based on calculated and experimental flow data, some important facts have emerged from the present analysis of a submersible hull with a bow thruster. Bow-thruster inflow does not seem to play a major part in bow-thruster jet interaction at vehicular ahead speed. Test results show that bow-thruster outflow is an important factor in bow-thruster jet interaction at vehicular ahead speed. The principal findings relative to this flow interaction based on an analysis of the test data are:

1. There was a persistent duct-outflow disturbance far downstream.
2. The pressure defect associated with thruster outflow was greatly reduced at high values of U_∞/U_j.
3. Relative duct size D/L was found to be important.
4. Extending the duct beyond the hull (in the form of a retractable pipe extension) was effective in reducing hull-suction effect.

A dimensional comparison that corresponds to approximately equal static-force conditions for equal ahead ship speed suggests that the outflow of a small high-velocity duct produces less interaction (suction) effect on the hull than does a large low-velocity duct when both are compared at the higher ahead ship speed.

ACKNOWLEDGMENTS

The author expresses his thanks to Mr. Curtis E. Shields, formerly of the Department of Hydromechanics and to the members of the Facilities Branch of the Department of Aerodynamics for their participation in the experimental program, as well as to Mr. Charles Dawson of the Department of Applied Mathematics for his contribution in running the LARC potential-flow program.

REFERENCES

1. Chislett, M.S. and Björheden, O., "Influence of Ship Speed on the Effectiveness of a Lateral-Thrust Unit," Hydro-og Aerodynamisk Laboratorium, Lyngby, Denmark, Report Hy-8 (Apr 1966).

2. Norrby, R., "The Effectiveness of a Bow Thruster at Low and Medium Ship Speeds," International Shipbuilding Progress, Vol. 14, No. 156 (Aug 1967).

3. Taniguchi, K. et al., "Investigations into the Fundamental Characteristics and Operating Performance of Side Thruster," Mitsubishi Technical Bulletin 35 (May 1966).

4. Feldman, J.P., "Model Investigation of Stability and Control Characteristics of a Preliminary Design for the Deep-Submergence Rescue Vessel (DSRV Scheme A)," David Taylor Model Basin Report 2249 (Jun 1966).

5. Stuntz, Jr., G.R. and Taylor, R.J., "Some Aspects of Bow-Thruster Design," Transactions Society of Naval Architects and Marine Engineers, Vol. 72 (1964).

6. Keffer, J.F. and Baines, W.D., "The Round Turbulent Jet in a Crosswind," Journal of Fluid Mechanics, Vol. 15, Part 4 (Apr 1963).

7. Jordinson, R., "Flow in a Jet Directed Normal to the Wind," Aeronautical Research Council, R&M 3074 (Oct 1956).

8. Hess, J.L. and Smith, A.M.O., "Calculation of Non-Lifting Potential Flow about Arbitrary Three-Dimensional Bodies," Douglas Aircraft Company Report ES-40622 (Mar 1962).

9. Schaub, U.W. and Cockshutt, E.P., "Analytic and Experimental Studies of Normal Inlets, with Special Reference to Fan-in-Wing VTOL Powerplants," Proceedings of the Fourth Congress of the International Council of the Aeronautical Sciences, Palais de l'Unesco, Paris (Aug 1964).

10. Addison, H., "Hydraulic Measurements," Second Edition, John Wiley and Sons, Inc., New York (1949), pp. 85-86.

UNCLASSIFIED

Security Classification

DOCUMENT CONTROL DATA - R & D

Security classification of title, body of abstract and indexing annotation must be entered when the overall report is classified)

1 ORIGINATING ACTIVITY (Corporate author) Naval Ship Research and Development Center Washington, D.C. 20007	2a. REPORT SECURITY CLASSIFICATION UNCLASSIFIED 2b. GROUP

3 REPORT TITLE

BOW-THRUSTER JET FLOW

4 DESCRIPTIVE NOTES (Type of report and inclusive dates)

Formal Research and Development Report

5 AUTHOR(S) (First name, middle initial, last name)

John L. Beveridge

6 REPORT DATE March 1970	7a. TOTAL NO OF PAGES 54	7b NO OF REFS 10
8a. CONTRACT OR GRANT NO b. PROJECT NO. S-F013 02 07 c. Task 1713 d.	9a. ORIGINATOR'S REPORT NUMBER(S) 3281 9b. OTHER REPORT NO(S) (Any other numbers that may be assigned this report)	

10. DISTRIBUTION STATEMENT

This document has been approved for public release and sale; its distribution is unlimited.

11. SUPPLEMENTARY NOTES	12 SPONSORING MILITARY ACTIVITY Naval Ship Systems Command

13. ABSTRACT

Interaction between the ambient flow of a hull and bow-thruster inflow and outflow is examined theoretically and experimentally. Pressure distributions for duct inflow were derived by potential-flow techniques, and wind-tunnel pressure tests and flow-visualization experiments were conducted to determine the characteristics of duct outflow. Generalized and specific results are presented and discussed for two sizes of circular ducts operating over a range of ratios of free-stream velocity to jet velocity.

DD FORM 1 NOV 65 1473 (PAGE 1)

S/N 0101-807-6801

UNCLASSIFIED

Security Classification

14 KEY WORDS	LINK A		LINK B		LINK C	
	ROLE	WT	ROLE	WT	ROLE	WT
BOW THRUSTERS						
Inflow						
Outflow						
FLOW INTERACTION						
Ahead Speed						